PL-TR-96-2225

DESIGN, EVALUATION, AND CONSTRUCTION OF TEXESS AND LUXESS, AND RESEARCH IN MINI-ARRAY TECHNOLOGY AND USE OF DATA FROM SINGLE STATIONS AND SPARSE NETWORKS: PHASE VI

Eugene Herrin
Paul Golden
Herbert Robertson

Southern Methodist University
Dallas, TX 75275 -0395

April 1996

Scientific Report No. 6

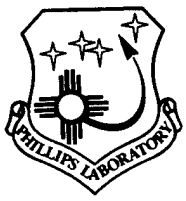

PHILLIPS LABORATORY
Directorate of Geophysics
AIR FORCE MATERIEL COMMAND
HANSCOM AFB, MA 01731-3010

SPONSORED BY
Advanced Research Projects Agency (DoD)
Nuclear Monitoring Research Office
ARPA ORDER No. 0325

MONITORED BY
Phillips Laboratory
CONTRACT No. F19628-93-C-0057

The views and conclusions contained in this document are those of the authors and should not be interpreted as representing the official policies, either express or implied, of the Air Force or U.S. Government.

This technical report has been reviewed and is approved for publication.

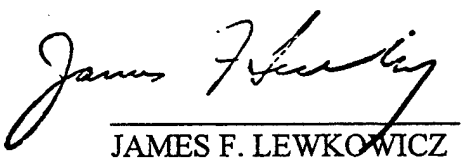

JAMES F. LEWKOWICZ
Contract Manager
Earth Sciences Division

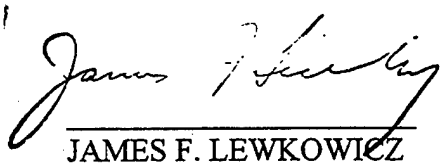

JAMES F. LEWKOWICZ
Director
Earth Sciences Division

This report has been reviewed by the ESD Public Affairs Office (PA) and is releasable to the National Technical Information Service (NTIS).

Qualified requestors may obtain copies from the Defense Technical Information Center. All others should apply to the National Technical Information Service.

If your address has changed, or you wish to be removed from the mailing list, or if the addressee is no longer employed by your organization, please notify PL/IM, 29 Randolph Road, Hanscom AFB, MA 01731-3010. This will assist us in maintaining a current mailing list.

Do not return copies of this report unless contractual obligations or notices on a specific document requires that it be returned.

REPORT DOCUMENTATION PAGE

Form Approved
OMB No. 0704-0188

1. AGENCY USE ONLY (Leave blank)	2. REPORT DATE	3. REPORT TYPE AND DATES COVERED
	April 1996	Scientific Report No. 6

4. TITLE AND SUBTITLE
Design, Evaluation and Construction of TEXESS and LUXESS & Research in Mini-Array Technology & Use of Data from Single Stations and Sparse Networks: Phase VI

5. FUNDING NUMBERS
PE: 62301E
PR NM93 TA GM WU AK

Contract F19628-93-C-0057

6. AUTHOR(S)
Eugene Herrin
Paul Golden
Herbert Robertson

7. PERFORMING ORGANIZATION NAME(S) AND ADDRESS(ES)
Southern Methodist University
Dallas, TX 75275

8. PERFORMING ORGANIZATION REPORT NUMBER

9. SPONSORING / MONITORING AGENCY NAME(S) AND ADDRESS(ES)
Phillips Laboratory
29 Randolph Road
Hanscom AFB, MA 01731-3010

Contract Manager: James Lewkowicz/ GPE

10. SPONSORING / MONITORING AGENCY REPORT NUMBER
PL-TR-96-2225

11. SUPPLEMENTARY NOTES

12a. DISTRIBUTION / AVAILABILITY STATEMENT
Approved for public release; distribution unlimited

12b. DISTRIBUTION CODE

13. ABSTRACT *(Maximum 200 words)*

Objectives are twofold: (1) to conduct research in seismic mini-array technology and use of data from single stations and sparse networks (CLIN 1), and (2) to design, evaluate, and construct two mini-arrays, TEXESS in Southwest Texas and LUXESS, northeast of Luxor, Egypt (CLIN 2) along the lines of a GSE Alpha Station. With de-installation on hold till diplomatic agreements are in place between the U. S. and Egypt for the installation of LUXESS, work has been directed to CLIN 1 research: love wave radiation from Central Texas quarry blasts, and the use of acoustic and seismo-acoustic data to identify vented explosive seismic sources.

14. SUBJECT TERMS	15. NUMBER OF PAGES
love wave radiation seismo-acoustic data vented explosive seismic sources	82
	16. PRICE CODE

17. SECURITY CLASSIFICATION OF REPORT	18. SECURITY CLASSIFICATION OF THIS PAGE	19. SECURITY CLASSIFICATION OF ABSTRACT	20. LIMITATION OF ABSTRACT
Unclassified	Unclassified	Unclassified	SAR

CONTENTS

CONTENTS

ILLUSTRATIONS

SUMMARY

Personnel contributing to this contract are: (1) Dr. Eugene Herrin, Principal Investigator, (2) Paul Golden, Director of Geophysical Laboratory, (3) Karl Thomason, Chief Engineer, (4) Nancy Cunningham, Director - Computer Laboratory, (5) David Anderson, Systems Analyst, (6) Dyann Anderson Slosar, Administration, (7) Herbert Robertson, Subcontractor, (8) Jack Swanson, Consultant, and (9) Dr. Gordon G. Sorrells, Subcontractor. Ph. D. students include: (1) Chris Hayward, (2) Relu Burlacu, (3) Jessie Bonner, and (4) Ileana Tibuleac.

Objectives

Objectives of the contract are twofold: (1) to conduct research in seismic-array technology and use of data from single stations and sparse networks, and (2) to design, evaluate, and construct two experimental arrays, TEXESS in Southwest Texas and LUXESS (Luxor Experimental Seismic System), which is northeast of Luxor, Egypt. These two tasks are dubbed CLIN 1 and CLIN 2.

The original CLIN 1 objectives were to: (1) conduct research in the use of single station and sparse network data in detecting and identifying small seismic events, (2) conduct research to develop optimum configurations and processing techniques for a nine-element experimental array, and (3) to continue development of an unmanned intelligent seismic station. These objectives have been revised by the Project Office in April 1994 as described on page 4 under Implications for Further Research. The contract has subsequently been revised to include acoustical research as a CLIN 1 objective.

CLIN 2 objectives are to: (1) acquire hardware and software, (2) install TEXESS, (3) perform site surveys and choose location for LUXESS, (4) test TEXESS and perform verification tests prior to de-installation, (5) de-install TEXESS, (6) complete civil work in Egypt, (7) install and test LUXESS, (8) de-install data acquisition, analysis and archiving equipment and ship to Helwan, Egypt, data center, and (9) install and test data acquisition, analysis and archiving equipment at Helwan data center. The contract is in the process of being extended to include additional tasks under CLIN 2 regarding the

establishment of the Egyptian array. TEXESS has recently been designated TXAR, which will be used when appropriate in the remainder of this report.

Technical Problem

The German Experimental Seismic System was dedicated in 1992 and represents an upgrade for regional arrays. Although GERESS was technologically advanced over NORESS and ARCESS, which were earlier regional arrays, because of greater sensitivity and wider dynamic range, there was a considerable effort that resulted in increased costs for pier and vault construction and trenching for power cabling. Now, in TXAR, innovations in emplacement techniques, such as the installation of sensors in shallow boreholes instead of vaults and the use of solar power at each site to eliminate cabling from a central-power source, have reduced array-installation costs by an order of magnitude. Other innovations are discussed below. TXAR is, therefore, a proposed design for a GSE-Alpha station because of these cost-cutting innovations. In addition to design, construction, installation, and operation of TXAR, research will be undertaken to develop new means of taking data and handling the data.

General Methodology

In GSE/US/84, February 1993, entitled "Technical Concepts for an International Data Exchange System," the GSE established the design goals of a future system. Goals are as follows:

1. Provide prompt access to all essential data
2. Provide convenient access to all available data
3. Provide direct access to all data at authorized national and global facilities
4. Accomplish goals with realistic manpower and budget resources.

The new concept of a global system for data exchange calls for an Alpha Network of 40-60 stations, primarily arrays; plus much greater than 60 Regional or Beta Stations; plus Local and National Networks or Gamma Stations.

SMU began research on experimental-array technology in 1991 on a previous contract. The proposed design was along the lines of an Alpha Station consisting of an array containing nine sites. Advancements over the GERESS design included the following:

1. The placement of seismometers and electronics in boreholes to greatly reduce construction costs for piers and vaults
2. The use of solar power at each site rather than a central-power source
3. The use GPS receivers for time data at each seismometer site to replace central timing from the Hub
4. The employment of radio links from seismometer sites to the Hub to replace cable links and associated construction costs
5. The use of modular equipment to facilitate the installation and maintenance of the array.

Four shallow boreholes about 7 meters deep and 11-5/8 in. in diameter were drilled and cased with standard 8-in. pipe. Special equipment and techniques were developed to lower and level seismometers in the boreholes. A prototype solar power array and directional antenna were also developed for installation at LTX.

Technical Results

The limited program described above was successful and SMU was granted a contract to design, evaluate, and construct two nine element experimental arrays: TEXESS and LUXESS.

Important Findings and Conclusions

The SMU mini-array research program that was begun in 1991 under the previous contract proved the feasibility of the proposed design and methodology described above.

Significant Hardware Development

Preliminary research has led to the following hardware developments:
1. The development of seismometer emplacement techniques in boreholes, including remote seismometer locking eliminated the need for vaults
2. Advancements in computer applications and radio modems allow all necessary electronic components to fit inside a 8-in. casing to provide physical protection and a more stable environment for the electronics
3. The use of Global Positioning Satellite (GPS) receivers to obtain timing accurate to within 10 ms of world time assuring time synchronization of the array
4. The use of modern digital radio modems allows the system to perform as a local area network referred to as a RAN (Radio Area Network); radio polling software provides wide bandwidth intra-array communications while requiring two base-station radios; the need for expensive buried fiber-optic cable is eliminated
5. A NEMA enclosure is mounted on top of the borehole and is used to house the batteries and as a mount for the solar-power array; the GPS receiver and radio antenna are mounted above it.

Special Comments

The task of adapting the solar-panel arrays at Lajitas to the LUXOR environment is simplified somewhat in that both TXAR and LUXESS are at approximately the same latitude, 30 deg North; both are in arid climatic zones; and both have about 3,500 annual hours of sunshine. As a result, there would be no need to modify the prototypic TXAR design because of differing environmental conditions at LUXESS.

Implications for Further Research

CLIN 1 objectives were revised by the Project Office in April 1994 to: (1) conduct research to develop optimum configurations and processing techniques for nine- and sixteen-element short-period arrays, (2) conduct research in discrimination of nuclear events using autoregressive (AR) modeling techniques on Lg data, and (3) conduct research in measuring 20-

second Rayleigh waves at regional distances using high-resolution, wide-dynamic-range, short-period, seismic-array data and broadband KS 36000 data.

CLIN 1 -- RESEARCH

Array Research

Conduct research to develop optimum configurations and processing techniques for nine- and sixteen-element short-period arrays,

In Scientific Report No. 1, PL-TR-94-2106, ADA284850, we discussed the problems of the large scatter of the order of ± 15 deg of azimuth estimates at GERESS after f-k processing. In order to address this problem, SMU research has concentrated on developing a time-domain processing technique to reduce this statistic using the nine-element TXAR array. The array-processing technique is similar to that described by Bernard Massinon in his paper entitled "The French seismic network -- current status and future prospects," which he presented at the GERESS Dedication and Symposium on 24 June 1992. The processing algorithm developed by SMU using GERESS D-ring data, which approximates the proposed 9-element TEXESS array, was presented in SMU-R-92-396, p. 14-17.

In Scientific Report No. 2, PL-TR-94-2258, ADA292546, array-processing research is described in Appendix 1. Specifically, Appendix 1 describes work on time-domain processing of GERESS and TXAR data to decrease azimuthal-error statistics with respect to that obtained by f-k processing. Time-domain processing has resulted in a reduction of azimuthal standard deviations from ± 15 degrees with f-k processing to ± 1.4 degrees with time-domain processing of TXAR data. The plan is to integrate the time-domain process with a detector that is being developed by Chris Hayward in order to automate array processing. Code is being developed as part of a joint-research project with Mission Research, Inc.

Calibration Studies

Calibration research at TXAR was addressed in Appendix A of Scientific Report No. 4, PL-TR-95-2091, ADA305417. A modified version of the correlation method described by Cansi, Plantet and Massinon in their 1993 paper entitled "Earthquake location applied to a mini-array: K-Spectrum versus correlation method" in *Geophysical Research Letters*, vol 17, p. 1819-1822 was used to estimate azimuth and horizontal phase velocity of 36 events recorded at TXAR for which we had USGS m_b values. Modifications to the correlation method include Fourier interpolation of the data by a factor of 8 to obtain a virtual sample rate of 320/sec, use of an L-1 technique (least absolute deviation) to obtain estimates of azimuth and phase velocity, and a moving window display to indicate those portions of the waveform that show strongest correlation across the array. Observed bias in estimated azimuth as large as 15° was found to be dependent on both distance and true azimuth.

This paragraph includes recent corrections not included in Appendix A of Scientific Report No. 4, Pl-TR-95-2091. Corrections have been forwarded to AFTAC and CMO. Based on 150 well located events (USGS), we have determined to the first order the attitude of the MOHO beneath TXAR to be:

Strike azimuth 111 deg (ESE)
Dip 10 deg north

This result is consistent with the tectonic setting for the area.

This structure leads to bias in estimates of back azimuth and phase velocity (or slowness) using TXAR arrival data. The following corrections should be made to the estimates:

Azimuth correction (dZ)
Add to the estimated back azimuth (Z') in degrees

$dZ = -7.44 \cos (Z'-111.2)$

Phase velocity correction (dV)
Add to the estimated phase velocity (V') in order to correct to the IASPI standard crustal model

$dV = - [0.44 + 0.86 \cos (Z' + 0.12)]$

We have also determined regional and teleseismic magnitude formulas for TXAR that are calibrated to mb (USGS) as follows:

For corrected phase velocity less than 8.6 km/sec:

$$m = \log A + 2.4 \log D - 3.95$$

For corrected phase velocity 8.6 km/sec or greater:

$$m = \log A + 2.4 \log D - 4.39,$$

Where A is maximum O - P amplitude in nanometers in the first 5 sec, and D is the epicentral distance in km.

Discrimination Research

Conduct research in discrimination of nuclear events using autoregressive (AR) modeling techniques on Lg data

In the framework of a Comprehensive Test Ban Treaty (CTBT), discrimination between low-yield or decoupled nuclear explosions, economic explosions and small shallow earthquakes using the characteristics of the seismic waves becomes very important. Some of the economic explosions are multiple-source events with a time and space pattern dependent upon the type of application. The superposition of the seismic motion in the time domain leads to regular amplification and suppression of spectral power in the frequency domain. As, in general, single events (single explosions or earthquakes) do not exhibit spectral modulations, their presence can be used in the discrimination between single and multiple events. The aim of the present study is to develop a fast and robust method of discriminating between earthquakes and economic explosions based on differences observed in the spectral content of the regional waveforms. The method is based on the parametric estimation of the power-spectral density (PSD) using the autoregressive (AR) Burg algorithm of order 3, which provides a fast method to emphasize the spectral differences.

In Scientific Report No. 2, PL-TR-94-2106, ADA284850, AR modeling is described in Appendices 2 and 4. The initial data set (see Table 1 of said report) includes about 30 mine explosions and earthquakes from the

Vogtland area of Czechoslovakia about 200 km northwest of GERESS. The frequency and reciprocal pole position of the complex pole in the AR (3) models were calculated using the Lg arrival for the Vogtland events recorded at GERESS in Table 1 of Scientific Report No. 3, PL-TR-95-2023, ADA295787. Figure 1 of Scientific Report No. 3, shows a clear separation of explosions and earthquakes with the latter having broad spectra with "weak" poles above 6 Hz whereas the explosions all show much "stronger" poles at frequencies less than 5 Hz. The AR (3) method appears to be an effective discrimant for small explosions and small earthquakes. Further work will be to answer questions regarding the method: (1) its effectiveness in other areas such as the Middle East, (2) its effectiveness using larger events, and (3) why the method works as well as it does?

Appendix A is a paper by Jessie Bonner entitled "Love Wave Radiation From Central Texas Quarry Blasts." This paper was prceded by a paper in Appendix A of Scientific Report No. 5 entitled "Azimuthal Variations of Rg Energy in Central Texas."

Conduct M_S:m_b research by measuring 20-second Rayleigh waves at regional distances using high-resolution, wide-dynamic-range, short-period, seismic-array data and broadband KS 54000 data.

The M_S:m_b discriminant has been investigated by a number of researchers for both regional and teleseismic events and explosions. Bases for the discriminant are (1) that explosions emit more energy in the form of high-frequency body waves and (2) that earthquakes emit more energy in surface waves having low frequency radiation; therefore, an Ms:m_b plot displays a significant separation of the two populations. The problem with the method is that of identifying small explosions; that is, the problem boils down to seismograph sensitivity. With the installation of new high-dynamic-range seismographs at TXAR, planned research includes the determination of Ms from small earthquakes at regional distances using the TXAR array data recorded by short-period GS-13 seismometers and a posthole, broadband KS 54000 seismometer. In Scientific Report No. 2, M_S:m_b studies were described in Appendices 3 and 4, and were excerpted in this section of Scientific Report No. 3, PL-TR-95-2023.

Acoustic Research

During the week of 21 September, a microbarograph pipe array was installed at TXAR, collocated with the posthole broadband system at the hub site, TX00. The array consists of six, 50-ft-long hoses, each with multiple ports, feeding into a common collector, dubbed the bomb, wherein the summed acoustic output is then fed into a single, solid hose containing a condenser microphone, which is suspended in a borehole. The microphone has been replaced by a pressure transducer, and its output is recorded on one channel of the CIM. Microbarograph data are being continuously transmitted to SMU for evaluation.

This is the first phase of a research program to analyze the origins of seismo-acoustic signals recorded at TXAR. Appendix B of Scientific Report No. 5 is a paper by Eugene Herrin and others entitled "Seismo-Acoustic Synergy." The research program is summarized by Gordon G. Sorrells in Appendix C of Scientific Report No. 5 in a paper entitled "Seismo-Acoustic Methods for the Detection of Acoustic Waves."

Appendix B of this report is a paper by Gordon G. Sorrells and Eugene Herrin entitled "A Preliminary Investigation of the Use of Acoustic and Seismo-Acoustic Observations to Identify Explosive Seismic Sources," which provides background information on detecting regional vented explosions in the Lajitas region.

Two additional microbarograph arrays were installed at TX02 and TX09 during the week of 24 March 1996 to form a tripartite microbarograph array with TX00.

CLIN 2 -- DESIGN, EVALUATION, AND CONSTRUCTION OF TXAR AND LUXESS

Experimental-Array Program

Information on the experimental-array program at SMU on the previous contract was presented in SMU-R-92-396, and in Scientific Report No. 1, PL-TR-94-2106, ADA284580.

TXAR AND LUXESS

Information on CLIN 2 has been presented in Scientific Report No. 1, PL-TR-94-2106, Scientific Report No. 2, PL-TR-94-2258, ADA292546, and Scientific Report No. 3. Since the submission of Scientific Report No. 3, an extension to the contract has been been granted to install LUXESS because of unavoidable delays. As a result, six additional tasks have been added.

Acquisition of Hardware and Software

The First and Second Quarterly R & D Status Reports cover the acquisition of hardware and software. TEXESS and LUXESS equipment are discussed in Scientific Report No. 1, PL-TR-94-2106. Instructions for the installation of the Posthole K-S54000 seismometer are presented in Appendix 5 of Scientific Report No. 2.

LUXESS equipment has been purchased and is being tested by Southwest Research Institute of San Antonio, Texas.

Array Hardware

Hardware is discussed in the Scientific Report No. 1, PL-TR-94-2106, ADA284580.

Computer Hardware

Computer equipment is discussed in the Scientific Report No. 1, PL-TR-94-2106, ADA284580.

Software

Acquisition of software was addressed in Scientific Report No. 1, PL-TR-94-2106, ADA284580.

Install TXAR

Layout

TXAR layout is discussed in Scientific Report No. 1, PL-TR-94-2106, ADA284580, and the relocation of C1 was discussed in Scientific Report No. 4, PL-TR-95-2091. Since then, the A, B, and C site prefixes have been superseded by TX prefixes as shown in Figure 1.

As mentioned in Scientific Report No. 4, information about TXAR, which has been compiled by Chris Hayward of SMU, can now be accessed on Internet via the World Wide Web at: http://inge.css.gov:65123/WebIDC/About_TXAR/

Installation

Installation is discussed in the Scientific Report No. 1, PL-TR-94-2106, ADA284580.

Perform Site Surveys and Choose Locations for LUXESS

As mentioned in Scientific Report No. 3, PL-TR-95-2023, two locations have been identified from satellite photos and maps for LUXESS, which are on granitic bodies located north of the road between Luxor and Quseir. Figure 4 of Scientific Report No. 3 is a digitally-enhanced LandSat image of the two

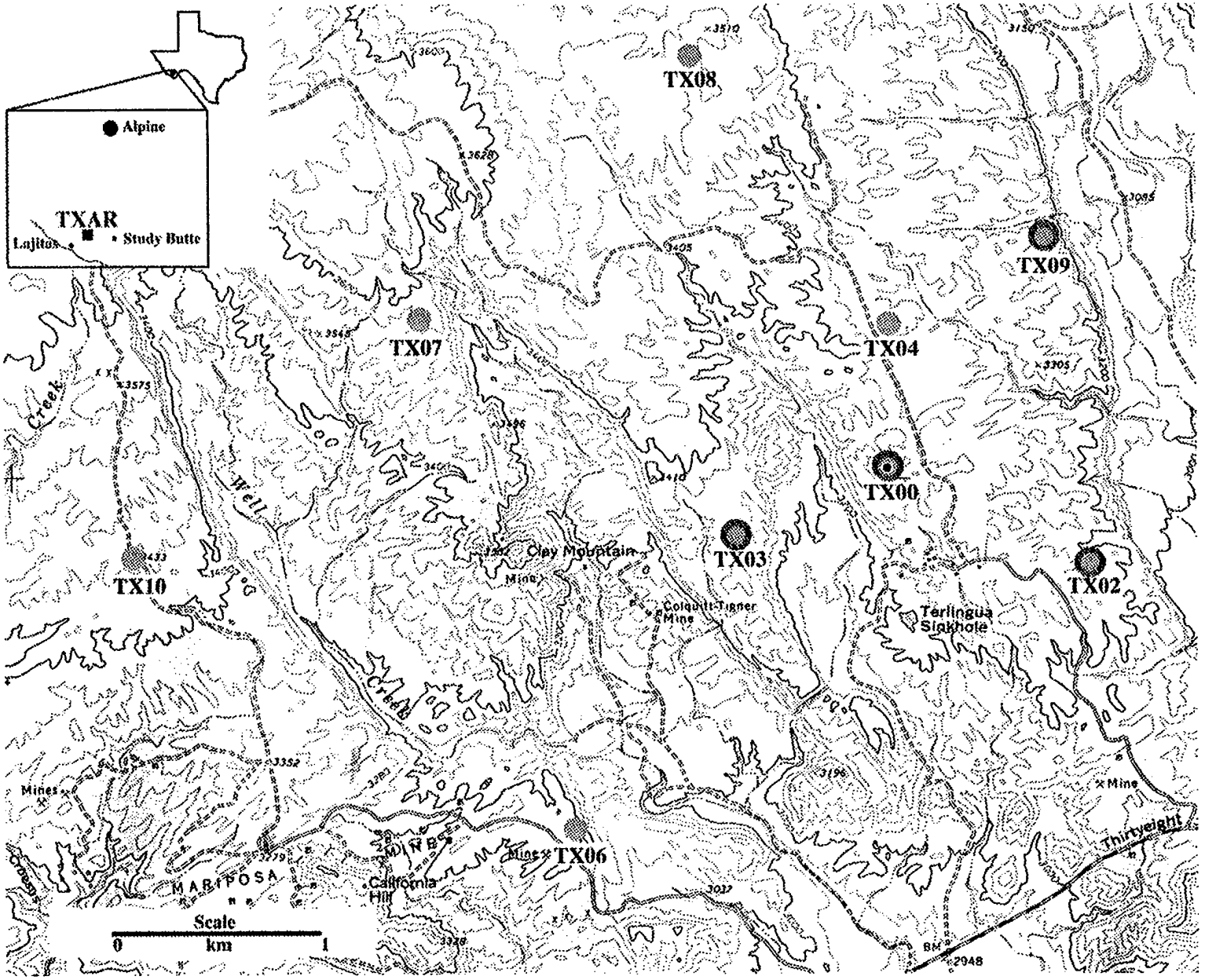

Figure 1. TXAR map showing new site designations.

circular granitic intrusions. The specific site for LUXESS will be selected by a team composed of SMU and Egyptian scientists.

Test TXAR Prior To De-installation

TXAR has been operational since 30 August 1993, but outages as discussed in this section of Scientific Report No. 3, PL-TR-95-2023, have led to reconfigurations as discussed in Scientific Report No. 4, PL-TR-95-2091, which should improve overall reliability.

Additional changes at TXAR have recently been made including CIM modification at TX01, AIM repair at TX07, installation of the microbaraograph array as mentioned previously, and site retrofit.

De-install TXAR

The present plan is to de-install all equipment except the seismometers, and transport said equipment to LUXESS. Equipment tagged for shipping includes the AIMs, radios, antennas, solar panels, batteries, NEMA enclosures, CIMs, and UPS.

Additional Tasks

Additional tasks such as training of Egyptian representatives, spare parts for LUXESS, and the broadband system were covered in Scientific Report No. 4, PL-TR-95-2091, pages 13 and 14.

Since then, three additional tasks have been approved by the Project Office as follows:

1. Perform research necessary to enhance the Air Force array in Belbasi, Turkey.
2. Perform research on the use of short-period vertical seismographs, collocated with pressure transducers, to provide seismo-acoutic synergy in the detection of acoustical waves from surface explosions.
3. Conduct cooperative research with Egyptian scientists to develop array processing software and hardware.

Visit of Russian Military Officials

Military representatives of the Russian Federation visited TXAR on 16 November 1995. Accompanied by U. S. Defense Department officials, the Russian representatives visited the station to study its design as part of their plans for the construction of similar stations in Russia. The SMU news release covering the visit is included as Appendix C.

APPENDIX A -- LOVE WAVE RADIATION FROM CENTRAL TEXAS QUARRY BLASTS

Jessie L Bonner

Introduction

A theoretical understanding of the source characteristics of ripple-fired chemical explosions is useful in determining the transportability of quarry blast discriminants from one region to another. The presence of short-period fundamental-mode Rayleigh waves (Rg), which are often observed on seismograms from explosions, is an indication of shallow source depth, therefore, Rg has been used as a depth discriminant in some regions (Kafka, 1990). Unfortunately, source characteristics can influence the Rg propagation such that Rg will not be seen on some blast seismograms (Goforth and Bonner, 1995). Further research has shown that the orientation of the topographic bench/open pit of a quarry influences the radiation pattern of Rg as shown in Figure A1 (Bonner, et al., 1996). For these reasons, Rg may not be as useful a discriminant as some other feature of the waveform.

On short-period seismograms in Central Texas, Love waves are most prominent at epicentral distances of 8 to at least 175 km where propagation paths traverse strata characterized by low-velocity sediments deposited during the Cretaceous period. Love waves from quarry blasts in Siberia suggest propagation extends to 500 km (Delitsyne, et al., 1996) increasing the usefulness of Love waves over Rg (Rg is rarely seen beyond 200 km) for a quarry blast discriminant.

Recent studies have noted interesting characteristics concerning Love waves generated by quarry blasts. Delitsyne and others (1996) studied thirty-two seismograms recorded 100 km from two quarries and found that Love waves are not generated on blasts without spall, the rock cast into the pit of the quarry. They also noted reversed Love wave patterns depending upon the orientation of the shots in the quarry. These results are summarized in Figure A2.

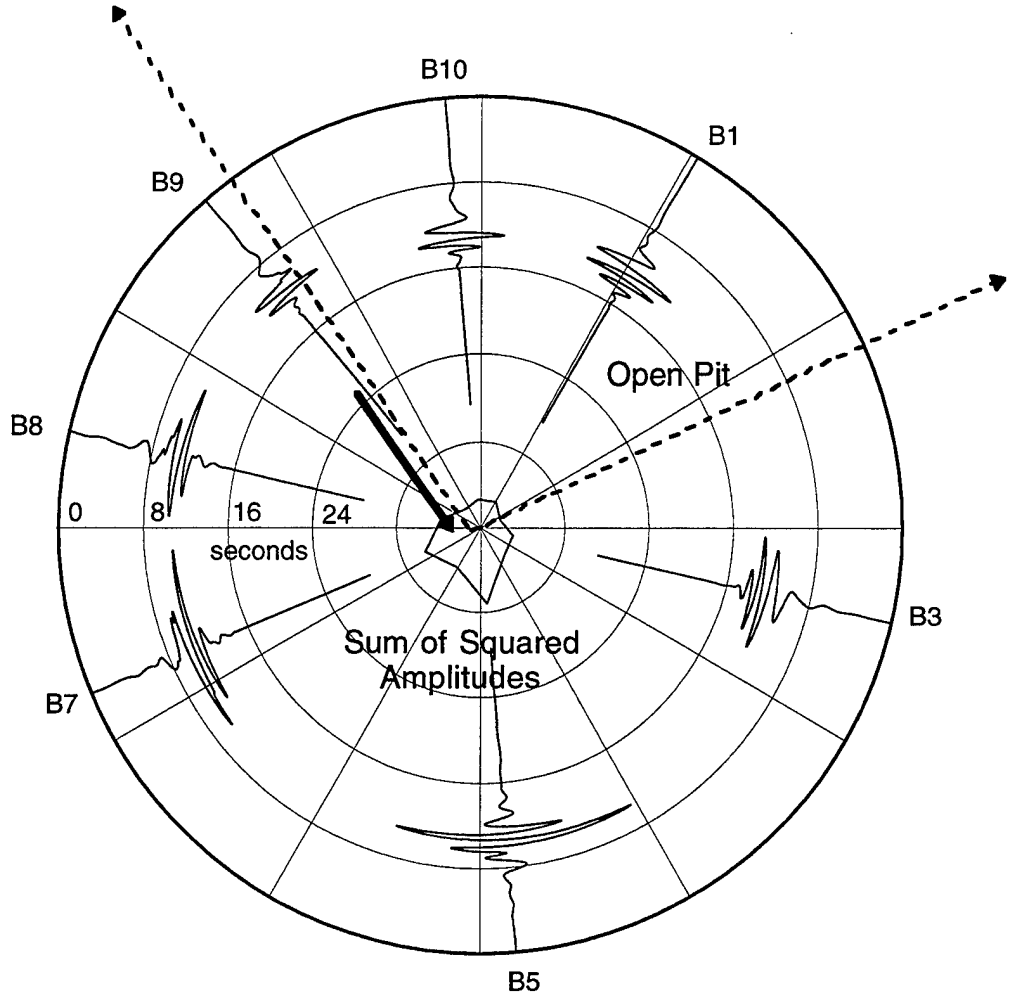

Figure A1. Azimuthal variation of Rg energy around the Chemlime quarry for the June 28, 1994 blast (Bonner, et al., 1996). Seismograms represent Rg, extracted from the vertical-component seismograms by phase match filtering, and are shown at the same amplitude and time scales. The dashed arrows represent the projection of the open pit of the quarry, while the interior plot shows the sum of the squared amplitudes for each trace. The solid arrow shows ripple fire orientation. Rg has more energy on paths that are behind the topographic bench (i.e. paths that do not travel through the open pit) of the quarry than along paths in front of the bench (i.e. paths that do travel through the open pit).

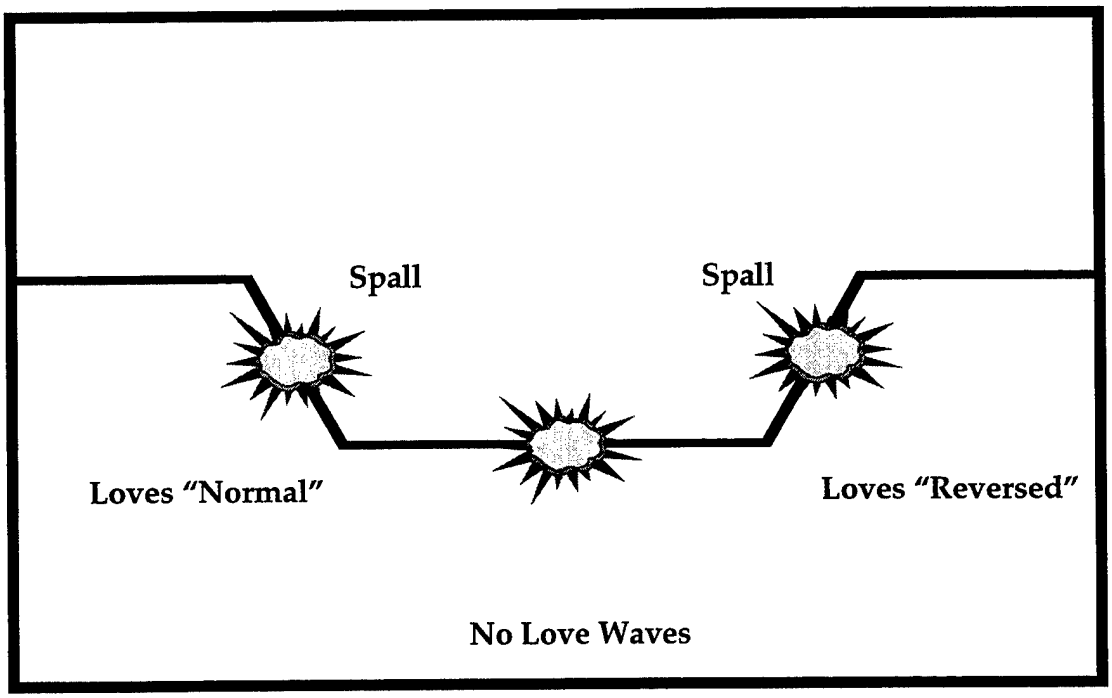

Figure A2. Quarry blasts recorded in Siberia show reversed Love waves depending upon the orientation of the shots in the quarry. Blasts conducted in the floor of the pit do not generate Love waves (Delitsyne, et al., 1996).

In this article, we investigated the transverse-component seismograms from explosions at the Chemical Lime (Chemlime) limestone quarry, 40 km west of Waco, Texas, by extracting Love waves from complex surface-wave trains. Relative energy in these extracted Love waves was then examined to determine azimuthal variations relative to the source characteristics. Dispersion curves were calculated by multiple filter analyses (MFA) (Herrmann, 1973; Dziewonski, et al, 1969), a single station method of determining group velocity dispersion. The dispersion curves were then used to extract Love waves from the waveform through the use of the phase-match filtering (PMF) technique (Herrin and Goforth, 1977). The relative energy in the extracted Love waves was then compared for different azimuths around the quarry.

Data Acquisition

This study used seismograms from three blasts at Chemlime on June 28, July 12, and July 17, 1994 (Table A1). The June 28 and July 12 blasts were detonated on a NW-SE trending (azimuth 325°) bench of limestone approximately 10 meters above the quarry floor (Figure A3). The July 17 detonation (Table A1) occurred on a wall approximately perpendicular to the previous one (azimuth 55°) in the same stratigraphic unit (Figure A3).

Table A1. Parameters for Chemlime quarry blasts

Blast Parameters	**28 Jun '94**	**12 July '94**	**17 Jul '94**
Number of holes	42	40	28
Total ANFO (lbs)	6964	6540	4856
Powder Factor	0.32	0.3	0.32
Rock moved (tons)	21,157	21,246	14,872

Seismograms were recorded on eight Sprengnether 6000 three-component, 2-Hz geophones connected to Reflection Technologies (REFTEK) DAS 72-0A systems. A Teledyne Geotech PDAS 100 system, placed at the quarry, recorded the origin time of each event using GPS hardware. Ten sites were selected to surround the quarry at a distance of approximately 10 km. At this distance, higher modes have separated from fundamental-mode surface waves enough

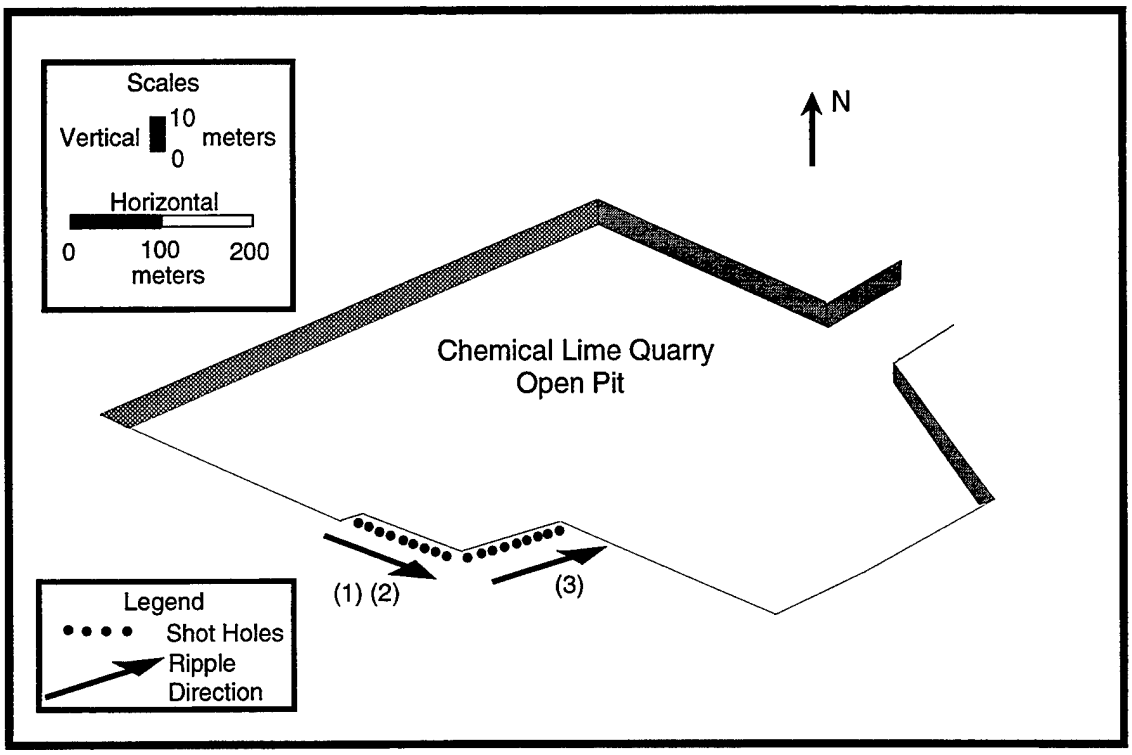

Figure A3. Schematic representation of the Chemical Lime (Chemlime) quarry pit 40 km west of Waco, Texas showing the approximate size and shape of the quarry. The stratigraphic unit being quarried is the Edwards Formation, a Cretaceous limestone approximately 10 m thick at this location. Three explosions were recorded from this quarry; (1) June 28, 1994 (2) July 12, 1994, and (3) July 17, 1994. The line of dots shows the direction of the ripple firing for each blast.

to allow adequate processing. Each site was selected based upon geology and site accessibility. All sites have several feet of well-defined soil to allow seismometer burial of 1-2 m, with the exception of B1, which was located in the rocky soils of the Edwards formation; therefore, it was buried at a depth of less than 1 m. Field logistics and accessibility resulted in a skewed network (Figure A4) with the seismometers ranging from 9.2 km (B7, B8, Figure A4) to 12.85 km (B10, Figure A4) from the quarry. At each site, the recorder was set to detect the quarry blast signals using a STA/LTA trigger. Disk failure at two sites (B6 and B4, Figure A4) reduced the active network to eight sites. Lack of triggering caused additional failures on the dates of the blasts, resulting in seven stations recording the June 28 (Figure A5) and July 17 explosions. For the July 12 blast, only six seismometers had been connected to the batteries (B1, B2, B7, B8, B9, B10, Figure A4) at the time of the early morning blast.

Sample rates were 100 samples per second for the June 28 blast, and 125 samples per second for the July 12 and July 17 blasts. The change was implemented because of possible aliasing of extremely high frequency P waves for the first blast on several stations. Fortunately, the bandwidth for short-period surface waves (0.4 to 2.5 Hz) was not compromised by this aliasing, and, in fact, the July 12 and July 17 records were eventually decimated to 100 samples per second to reduce computational time. Because the Love wave bandwidth includes the 2 Hz (0.5 seconds period) instrument corner frequency where the maximum phase shift occurs, both amplitude and phase corrections were applied prior to phase-matched filteringThe correction was made by dividing the complex Fourier transform (FT) of the signal by the complex seismometer response. The inverse FT of the result, after correction to ground motion velocity (cm/sec), is the corrected waveform used in the study.

Data Processing

Phase Identification

Transverse-component seismograms from the June 28 blast show the complex nature of the quarry blast signals at approximately 10 km distance (Figure A6). Applying a high-pass filter to each component allows detection

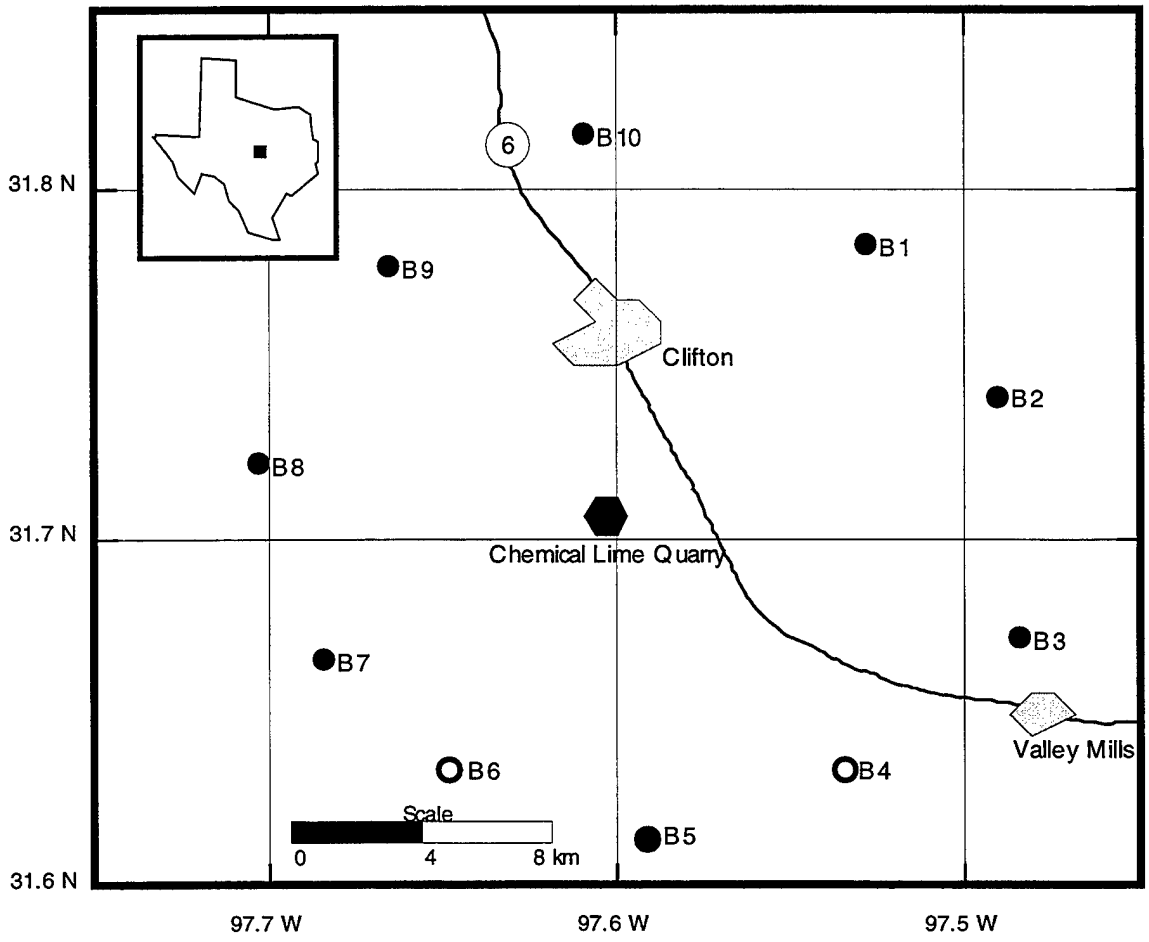

Figure A4. Portable network of seismometers used to record three chemical explosions from the Chemlime quarry. Stations B4 and B6, represented by open circles, were inoperable during the experiment due to hard disk failure.

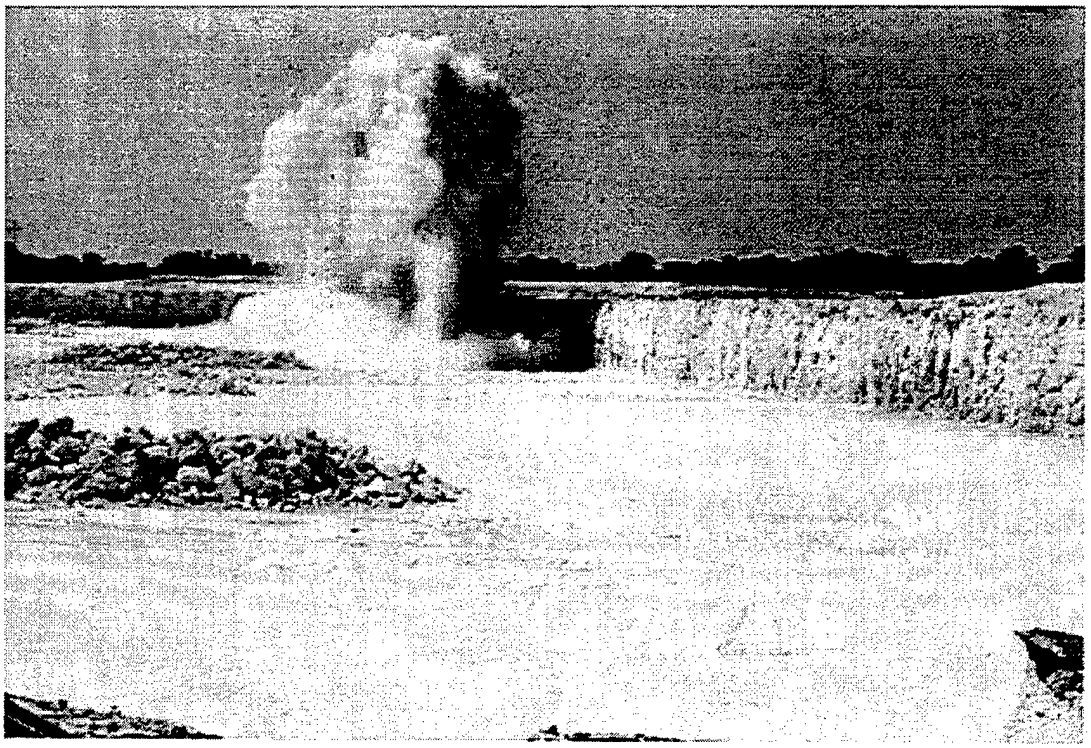

Figure A5. The June 28, 1994 Chemlime Explosion. For scale, the height of the topographic bench is approximately 10 meters.

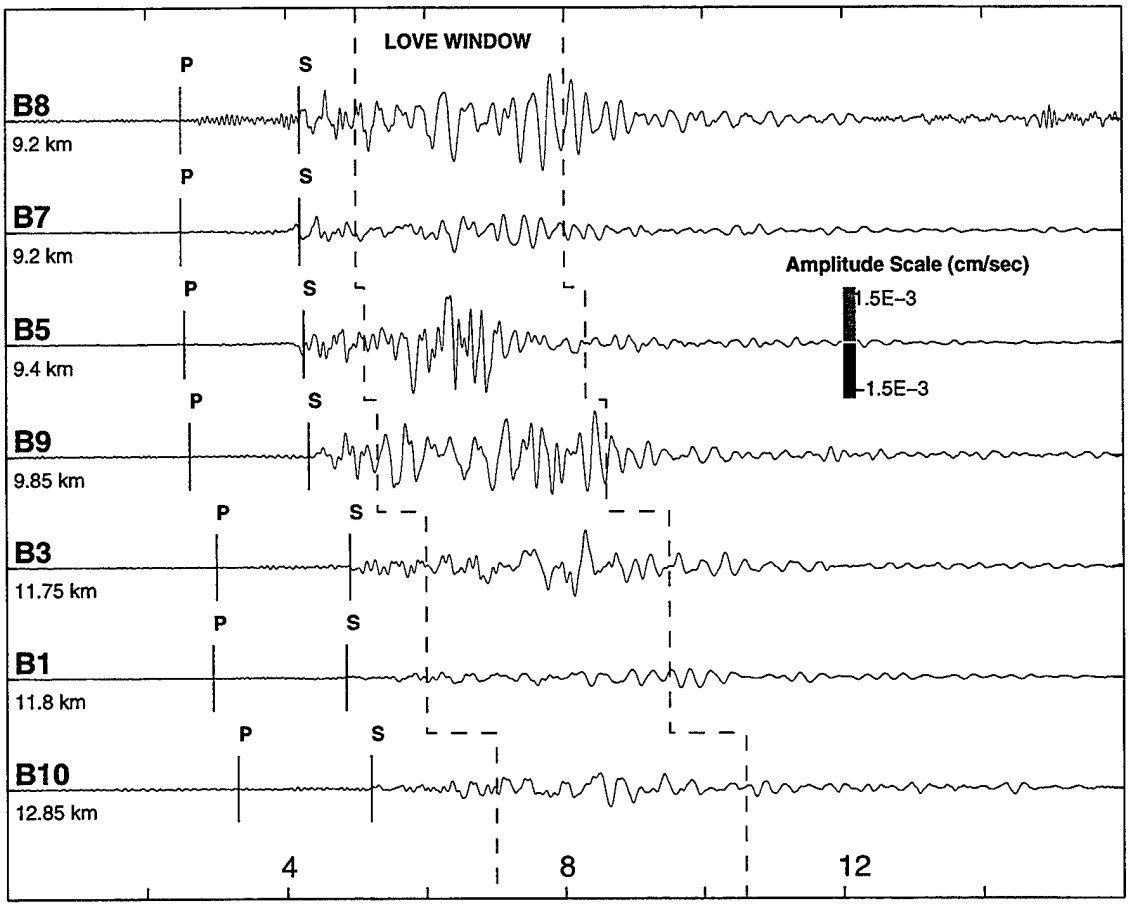

Figure A6. Transverse component seismograms corrected to velocity (cm/sec) for the instrument response from the June 28, 1994 Chemlime explosions shown at the same amplitude and time scales. The waveforms are plotted as a function of distance from the quarry. At this distance, Love waves are not well defined, due to the presence of coda, higher modes, and other arrivals, unless bandpass filtering is done in the appropriate bandwidth (0.4 to 2.5 sec period).

of the high-frequency P waves. These arrivals have group velocities ranging from 2.5 to 3.0 km/sec, less than the velocities (3.8 to 4.2 km/sec) determined for the upper crust of Central Texas (Bonner, 1993). This undoubtedly is the result of shorter propagation paths (i.e., shallower penetration depths) in this study. The group velocities of Pg arrivals in Bonner (1993) are in accordance with values for sedimentary rocks in Oklahoma (Trygvasson and Qualls, 1967). Seismograms for the July 12 and July 17 blasts are presented in Figures A7 and A8, respectively.

Shear wave phases are impulsive on the transverse components and mark the beginning of a complex assemblage of higher mode and fundamental-mode Love waves, accompanied by multipathing arrivals. Group velocities for the S waves range from 1.7 to 2.2 km/sec, while group velocities for the surface waves were calculated by Multiple Filter Analyses.

Dispersion Analysis

The Multiple Filter Analysis technique (MFA), first developed by Dziewonski, et al. (1969), and implemented using a set of computer programs written by Robert Herrmann, provides a fast, efficient method of analyzing multiply dispersed signals. In this method, a set of narrow band Gaussian filters is applied to the input spectra at certain period intervals. The envelope of each filtered time signal is then searched for the occurrence of the four largest envelope amplitudes. Each of these amplitude maxima occurs at an associated time from the origin of the event, and when combined with the distance from the quarry, a group velocity can be estimated for each arrival (Herrmann, 1973). These amplitudes are then normalized, contoured, and displayed on a plot of group velocity versus period. Analysis was restricted to periods between 0.23 and 3.0 seconds. For periods below 0.23 seconds, the surface wave train analysis is complicated by interference from the S-wave coda, while periods greater than 3.0 seconds are influenced greatly by microseisms and instrument noise. The dispersion curves obtained by Multiple Filter Analyses of the vertical and transverse components of B9 are shown in Figure A9.

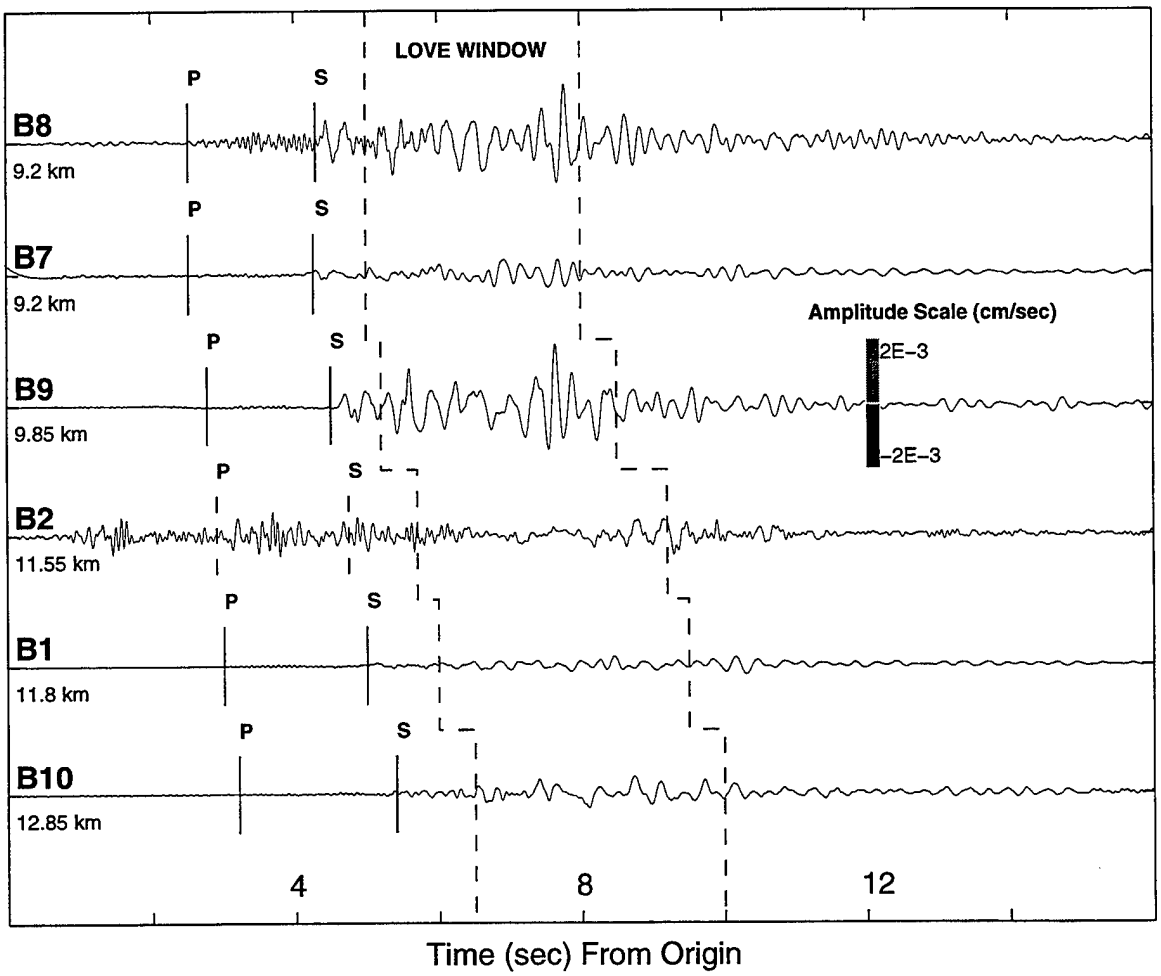

Figure A7. Transverse component seismograms corrected for instrument response from the July 12, 1994 Chemlime explosion shown at the same amplitude and times scales.

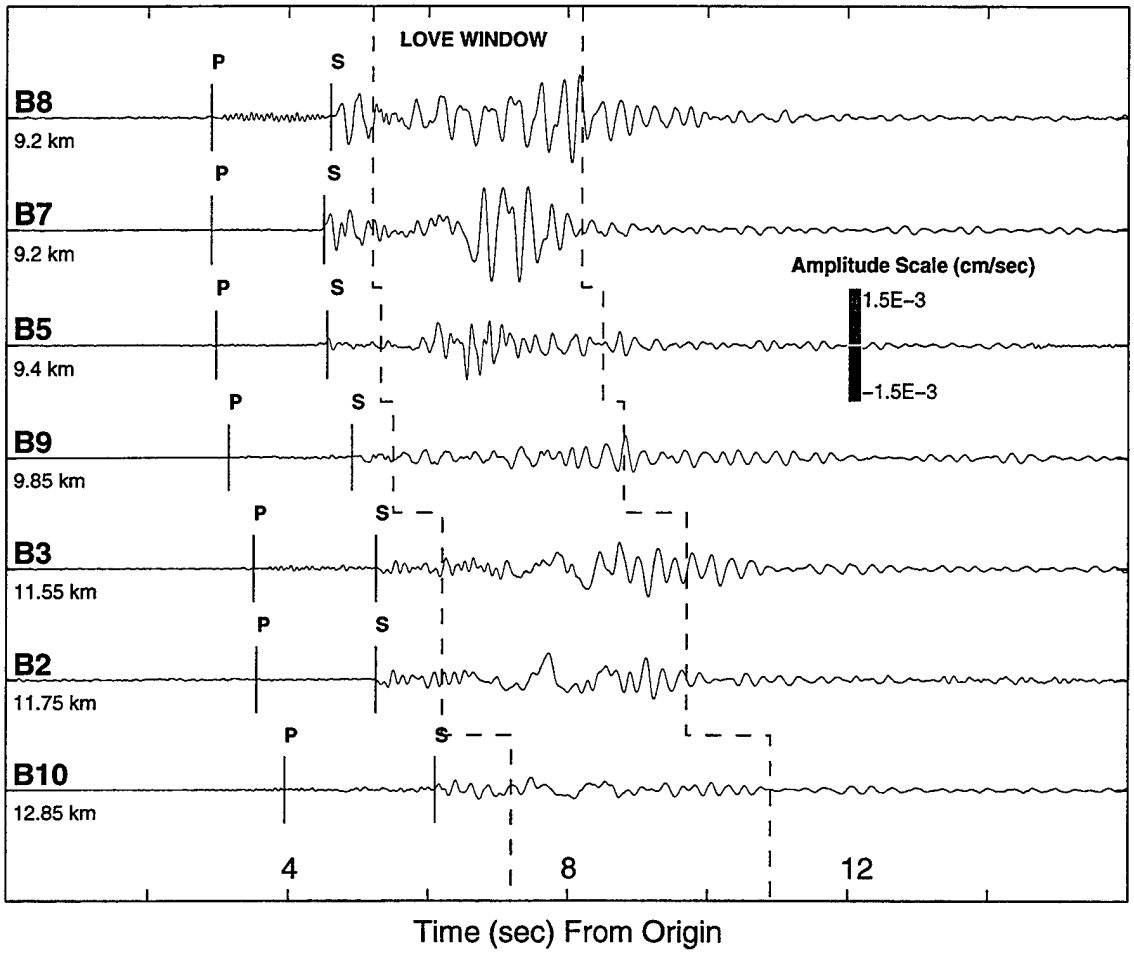

Figure A8. Vertical component seismograms corrected to instrument response from the July 17, 1994 Chemlime explosion shown at the same amplitude and time scales.

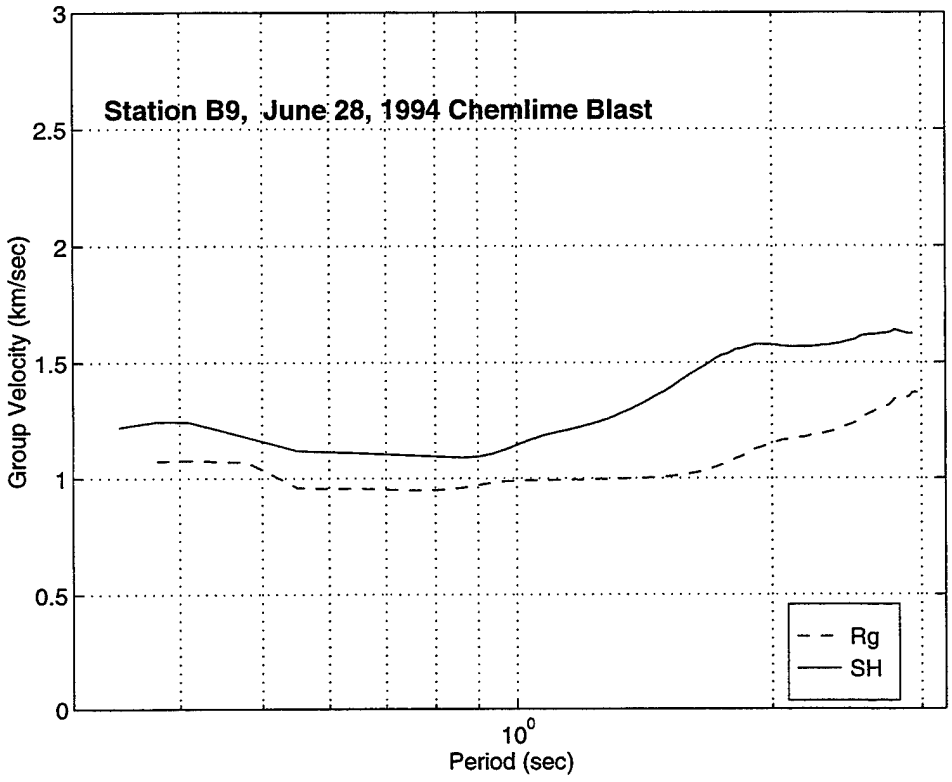

Figure A9. Rg and Love wave dispersion curves for the June 28, 1994 blast recorded at station B9. Dispersion curves were interpreted through results of the multiple filter analysis of the vertical (Rg) and transverse (Love) components.

Phase Match Filtering

The dispersion curves carefully interpreted by MFA serve as the input to the phase match filtering (PMF) technique (Herrin and Goforth, 1977). The PMF procedure starts with an initial estimate of dispersion and by an iterative technique finds and applies a filter that is phase-matched to the particular mode or arrival of a surface wave-- Love in this study. With the Love arrival separated, the relative energy in Love can then be calculated.

Cross-correlation of a signal s(t) with a filter f(t) can be represented in the frequency domain as:

$$s(t) \otimes f(t) = | S(\omega) | | F(\omega) | e^{(i(\delta(\omega)-\sigma(\omega)))},$$

where $\delta(\omega)$ and $\sigma(\omega)$ are the phase spectra of s(t) and f(t) respectively, and S(ω) and F(ω) are the amplitude spectra. If f(t) is chosen such that the Fourier phase is the same as that of s(t), then f(t) is a phase-matched filter with respect to s(t). For a more complete discussion of the PMF technique, the reader is referred to Herrin and Goforth (1977), who originally applied this class of linear filter to surface waves. The advantage of using the PMF is that the final results are less contaminated by higher modes and multipathing arrivals. Thus, the complex spectrum of the primary signal can then be recovered from multiple arrivals. With this in mind, the PMF represents a method of extracting Love waves from the waveform in order to establish any azimuthal variations in the energy of Love waves.

Problems exist in using the PMF technique on Love waves that do not exist with similar analyses of vertical components for Rayleigh waves (Goforth and Herrin, 1979). Not only does Love multipathing contaminate the surface-wave train, but so does Rayleigh multipathing. Also, Love waves often arrive at a recording station from an azimuth differing significantly from that of the primary Rayleigh. The result of these two manifestations is contamination of the Love-wave train. For this study, these problems are considered minimal due to the short propagation path between quarry and station.

Results

Spectral Comparisons

Power spectra were calculated for all signals recorded during the duration of the experiment. Each FT consists of time-domain signal beginning 2 seconds before the onset of the first arrival (P) and continued for 20 seconds (total of 2000 sample points). The total length of the FT was 2048 points with a 256-point Bartlett window applied to smooth the spectra. The spectral comparisons for all stations recording the Chemlime blasts are presented in Figures C10-C17. Each plot shows the power spectrum magnitude, in dB, relative to 1 cm/sec ground velocity. The horizontal axis is frequency, in Hz, and ranges from 0.4 to 15 Hz for each plot.

Comparisons for station B1 (Figure A10) consisted only of the June 28 and July 12 spectra. As noted in Table A1, both blasts had similar blasting parameters and occurred along the same wall of the quarry. Even though the June 28 blast involved slightly more explosives, the July 12 blast spalled more material into the quarry. As a result, the spectra for both blasts are similar. This similarity, in the absence of cultural noise (i.e. Texas Longhorn cattle and farm equipment), is noted for all stations recording both June 28 and July 12 blasts (B7, Figure A14; B8, Figure A15; B9, Figure A16; B10; Figure A17). In most cases, the June 28 Chemlime blast has slightly more energy in the Love wave bandwidth (0.4 to 2.0 Hz) than does July 12.

The first evidence that a radiation pattern exist for Love waves generated by ripple-fired quarry blasts become evident from analyzing the spectral content of station B2, where both the July 12 and July 17 blasts were recorded. Unlike the similarity of the June 28 and July 12 spectra for some stations, strong differences in spectral magnitude between these blasts is observed (Figure A11). We might interpret the differences to be related to the amount of explosives used, and in doing so we would conclude the July 17 blast to be larger in size than the July 12 blast. However, this was not the case (Table A1), for the total explosives used for the July 17 blast was over 25% less than for July 12 and June 28. Similar spectral comparisons were made for B3 (Figure

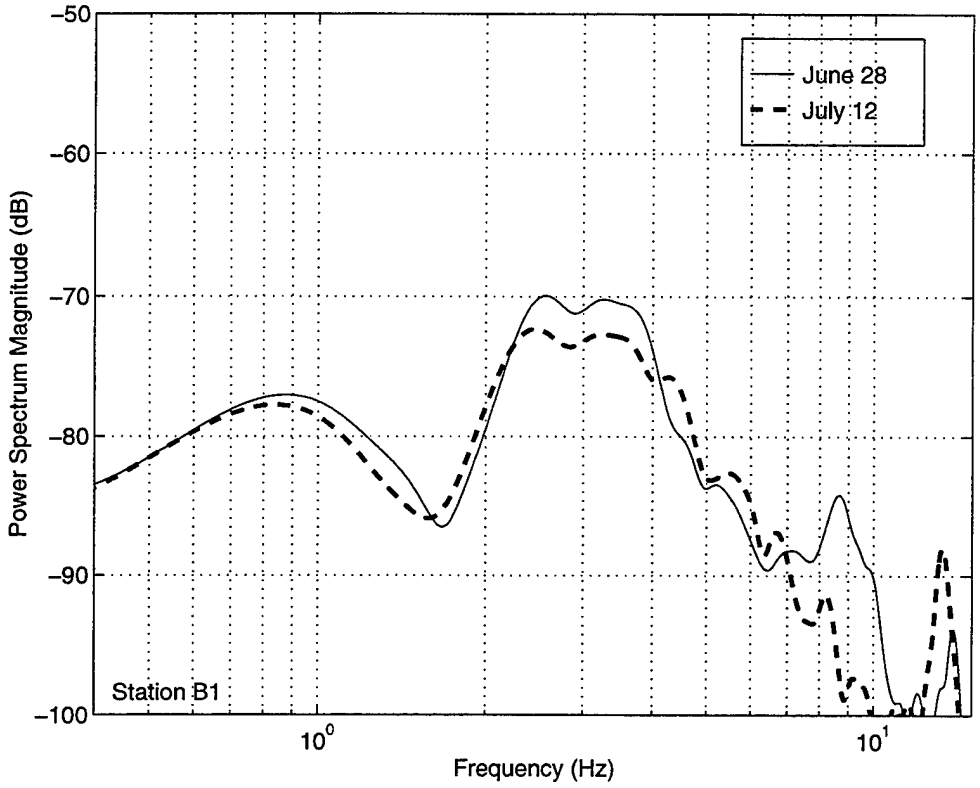

Figure A10. Spectral comparison of the June 28 and July 12, 1994 Chemlime quarry blasts recorded at B1. The vertical scale is dB relative to 1 cm/sec ground velocity, and spectra consist of 20 seconds of transverse component data, starting 2 seconds before the onset of P. Spectra are similar since both blasts occur along the same wall and are approximately equal in size (Table 1).

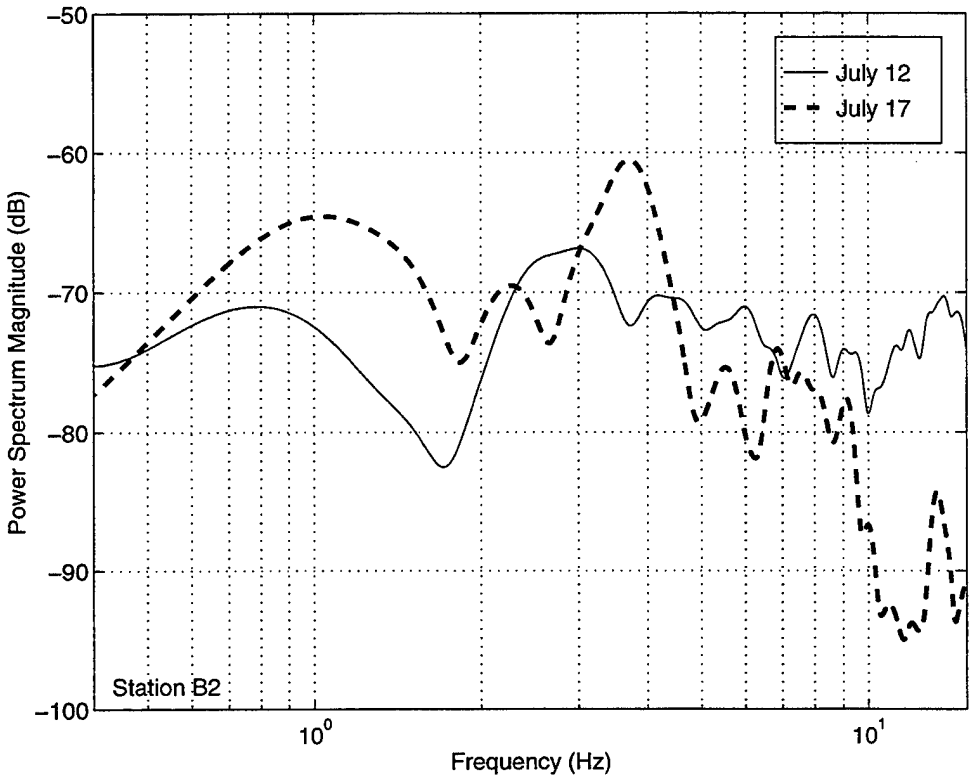

Figure A11. Spectral comparison of the July 12 and July 17, 1994 Chemlime quarry blasts recorded at B2.

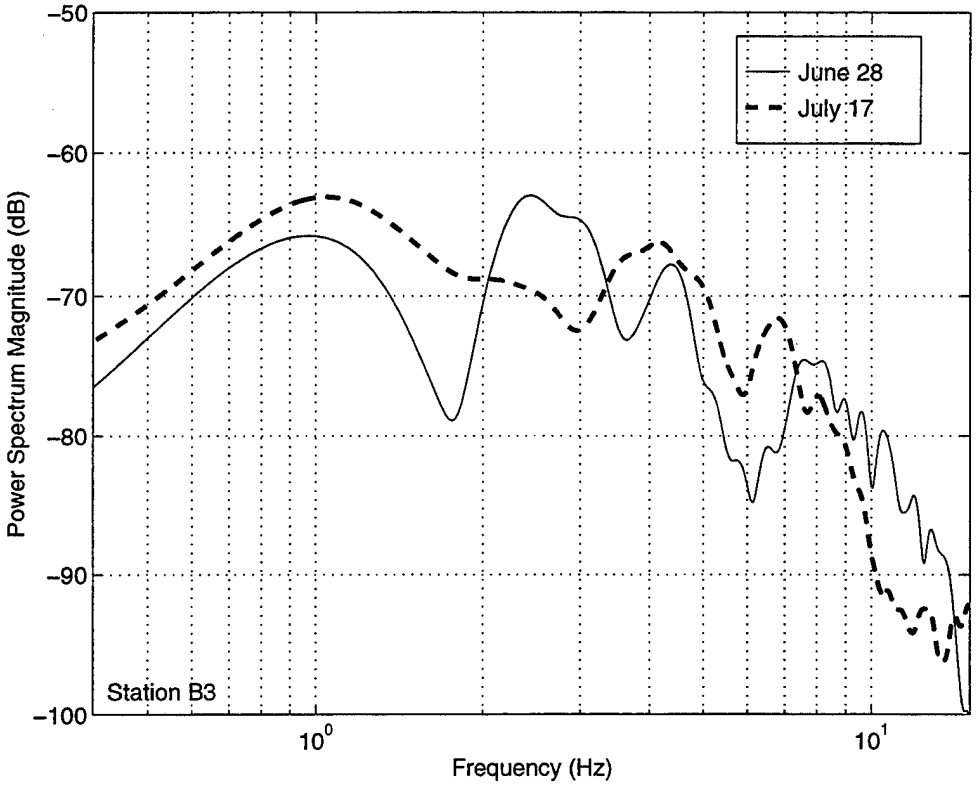

Figure A12. Spectral comparison of the June 28 and July 17, 1994 Chemlime quarry blasts recorded at B3.

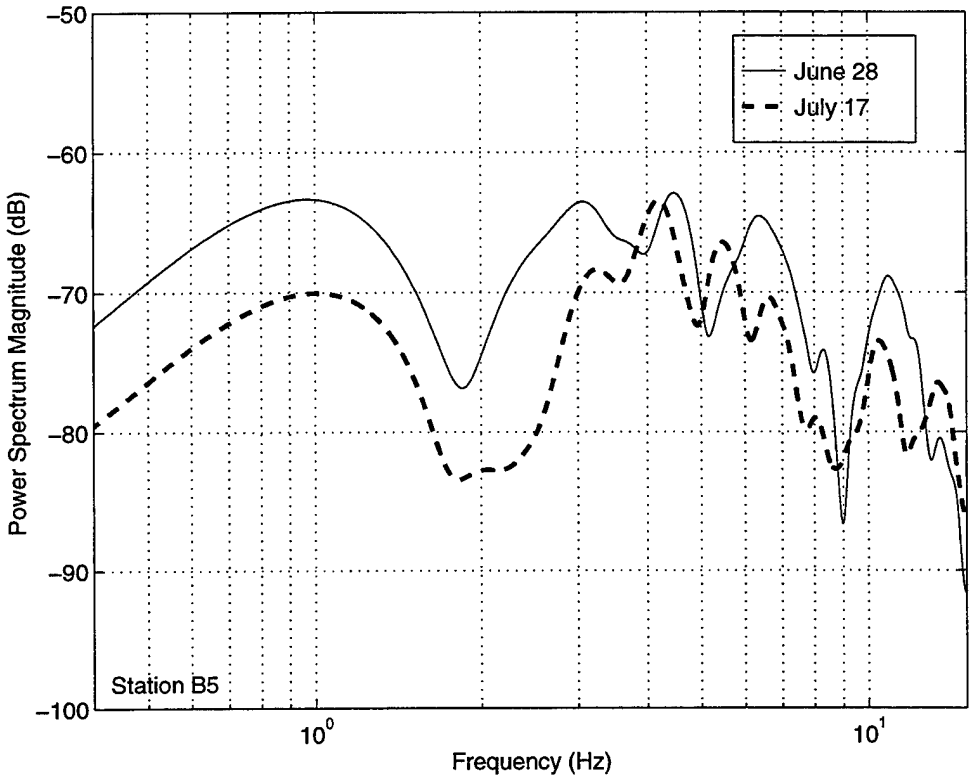

Figure A13. Spectral comparison of the June 28 and July 17, 1994 Chemlime quarry blasts recorded at B5.

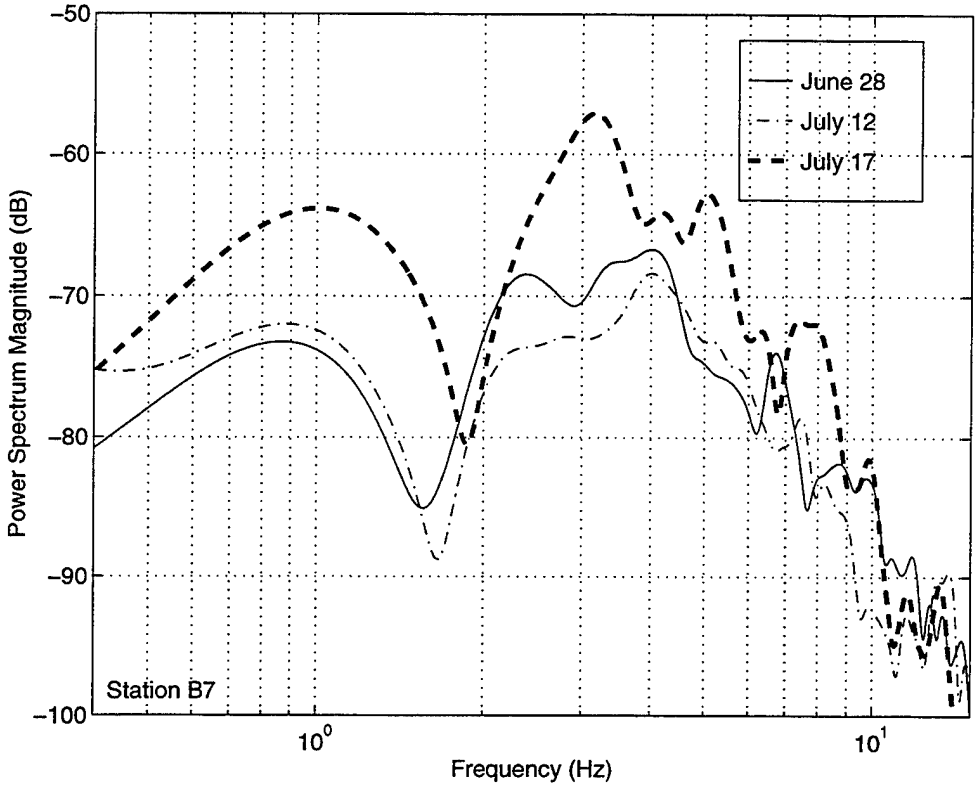

Figure A14. Spectral comparison of the June 28, July 12, and July 17, 1994 Chemlime quarry blasts recorded at B7.

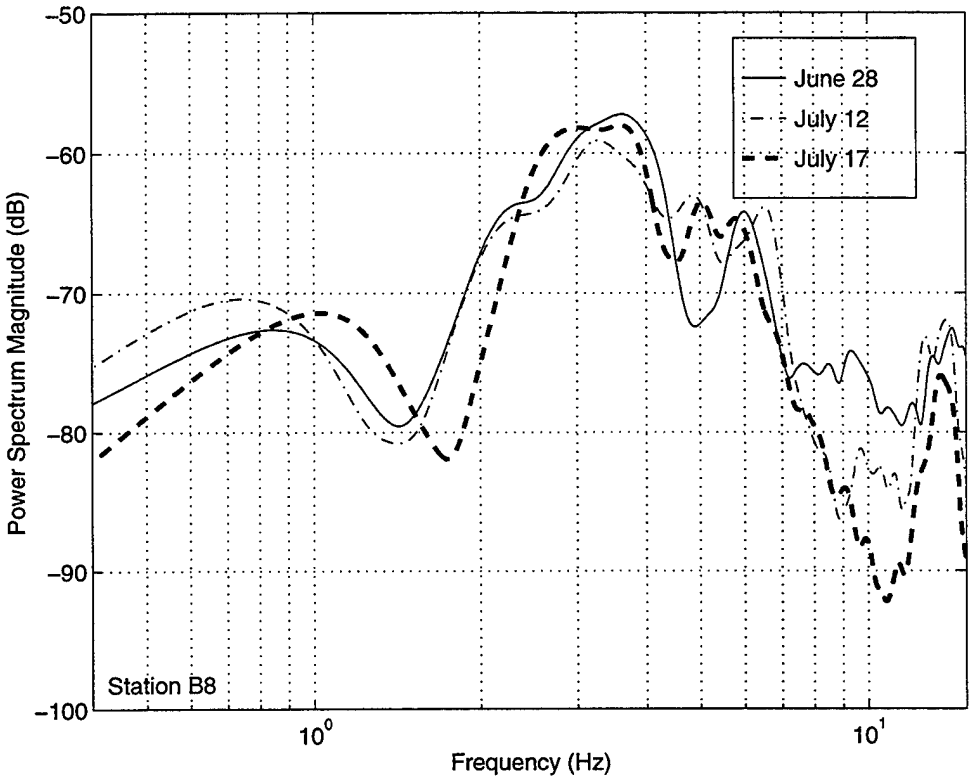

Figure A15. Spectral comparison of the June 28, July 12, and July 17, 1994 Chemlime quarry blasts recorded at B8.

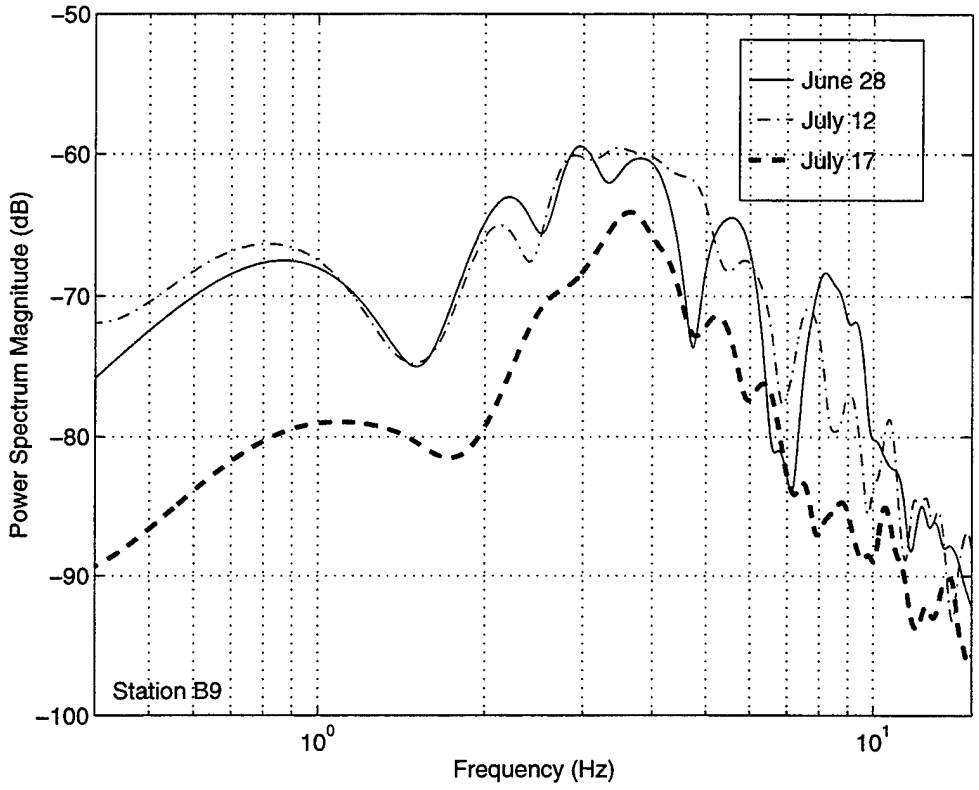

Figure A16. Spectral comparison of the June 28, July 12, and July 17, 1994 Chemlime quarry blasts recorded at B9.

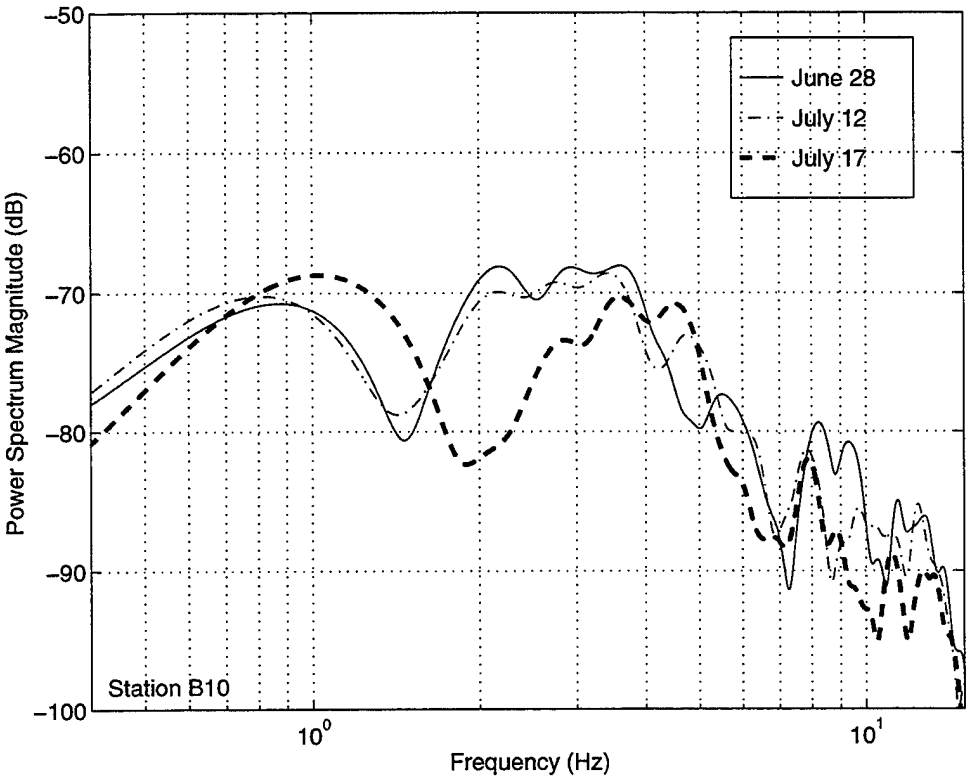

Figure A17. Spectral comparison of the June 28, July 12, and July 17, 1994 Chemlime quarry blasts recorded at B10.

A12), and B7 (Figure A4). Other spectra show that the July 17 blast was indeed smaller than the first two (B5, Figure A13; B9, Figure A16), while the spectra estimated at stations B8 and B10 (Figure A15 and Figure A17, respectively) predict three similar blasts. Obviously, the source was contributing to these spectral differences by creating azimuthal variations in Love wave radiation.

Azimuthal Variations of Love Energy

Love waves for all three blasts extracted by phase-matched filtering are shown in Figures A18-A20, scaled to the same amplitude and time scales. Obviously, some traces have a larger amplitude than others, but with this type of plot, azimuthal variations are hard to establish. These same seismograms are plotted in a polar representation in Figures A21-A23 that better distinguishes how the Love wave energy is varying with azimuth. Each plot has the projection of the open pit of the quarry (dashed arrows) and the direction of the ripple (solid arrow) superimposed on it. The time scale is in seconds from the origin of the blast and starts at the edge of the graph, with time increasing toward the center. An important part of the graph is the interior plot, which is an outline of the sum of the squared amplitudes in the Love wave signals.

A double-lobed propagation pattern for Love waves generated by ripple-fired explosions at Chemlime is noted by studying the interior plots of Figures A21-A23. The long axis of this "peanut" shaped pattern is oriented parallel to the direction of ripple firing, and in changing the working bench, the long axis is reoriented to reflect this change (Figure A23). Also, more energy is recorded in the direction of the ripple and behind the topographic bench, creating two lines of asymmetry in the lobes (Figure A24). Based upon these results, both the orientation of the topographic bench and ripple-fire direction influence the radiation of Love waves.

Concluding Remarks

Love wave radiation patterns recorded in this study show correlation with the orientation of the bench and with the ripple-fire direction. Figure A25 shows initial results of of finite difference calculations (McLaughlin and Bonner, 1996) that model the Chemlime quarry predict SH patterns consistent

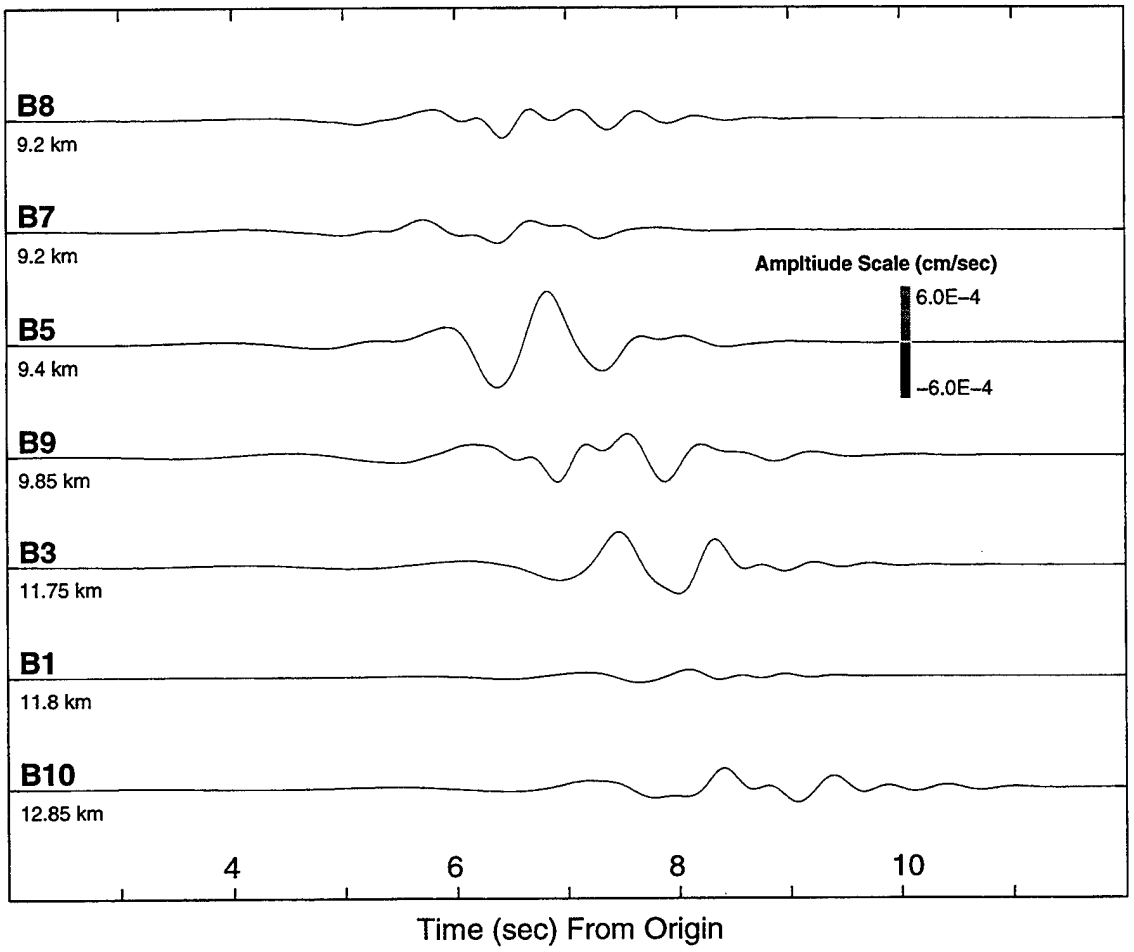

Figure A18. PMF extracted Love waves from the June 28, 1994 Chemlime explosion, band-pass filtered in the forward and reverse directions between 0.4 and 2.0 Hz. Traces are presented at the same amplitude and time scales.

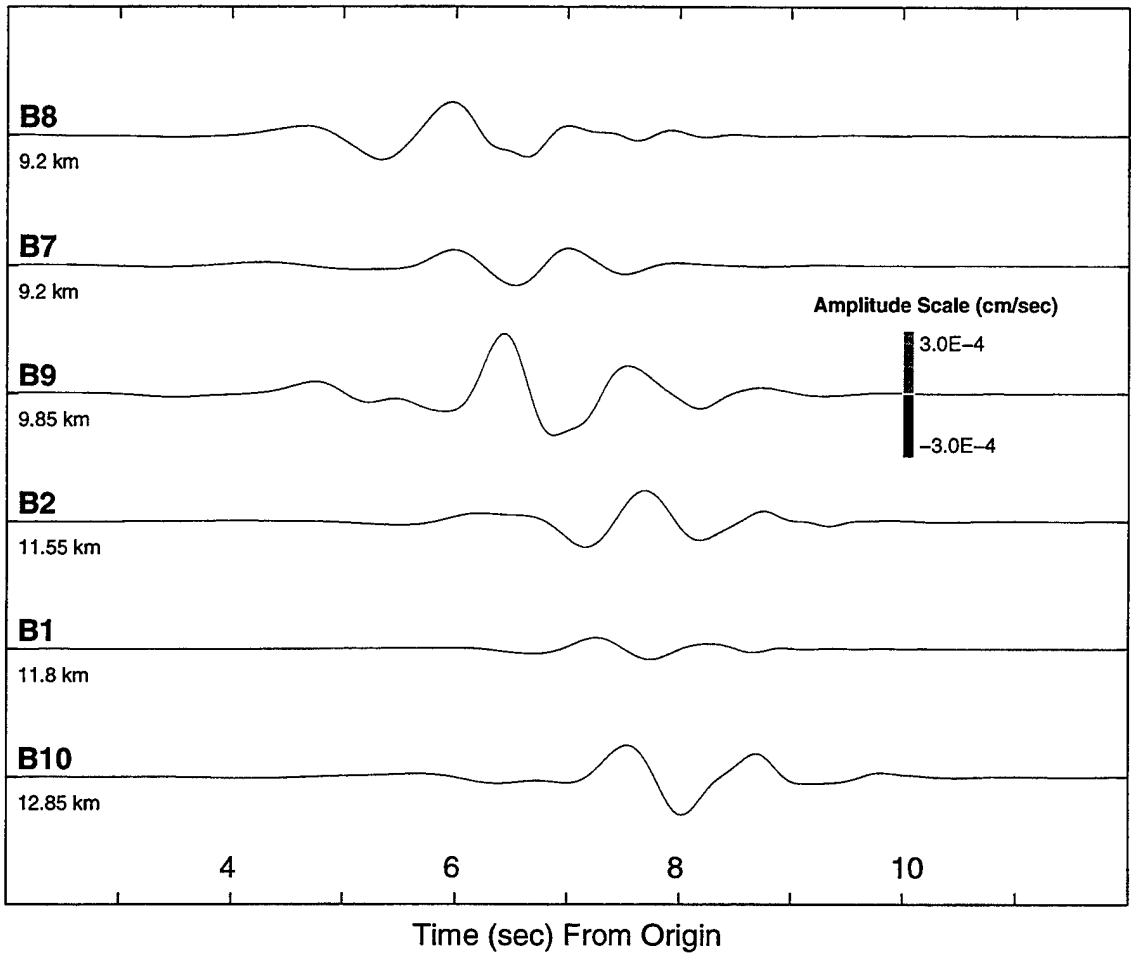

Figure A19. PMF extracted Love waves from the July 12, 1994 Chemlime explosion, band-pass filtered in the forward and reverse directions between 0.4 and 2.0 Hz. Traces are presented at the same amplitude and time scales.

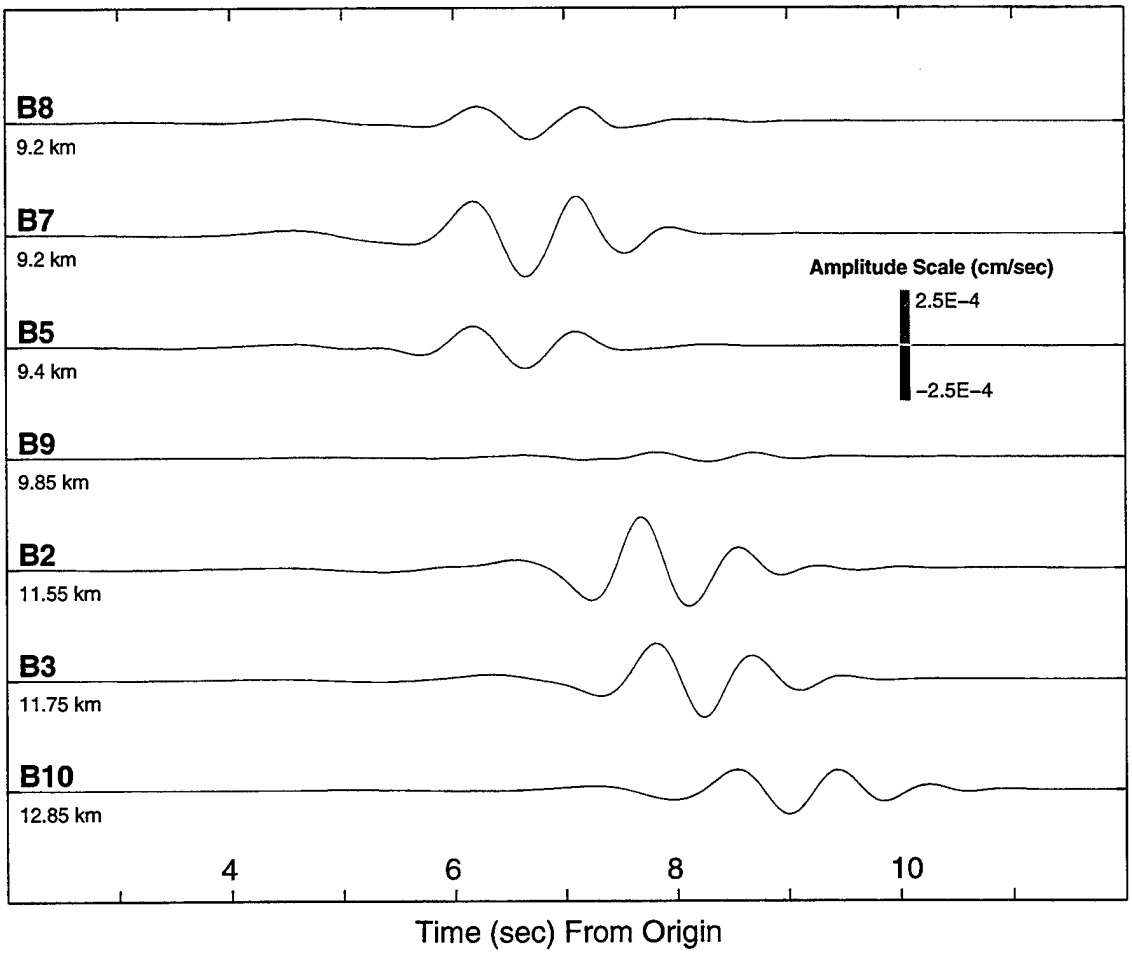

Figure A20. PMF extracted Love waves from the July 17, 1994 Chemlime explosion, band-pass filtered in the forward and reverse directions between 0.4 and 2.0 Hz. Traces are presented at the same amplitude and time scales.

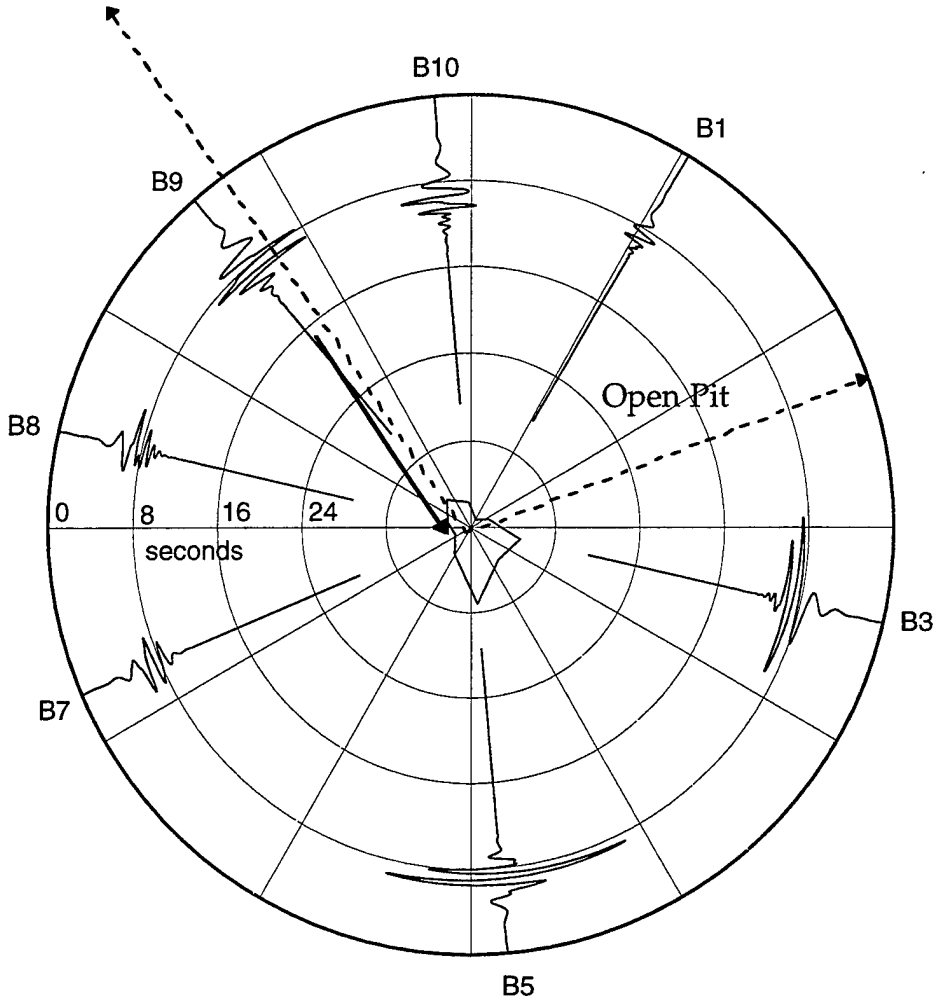

Figure A21. Azimuthal variation of Love wave energy around the Chemlime quarry for the June 28, 1994 blast. Seismograms represent Love waves, extracted from the vertical-component seismograms by phase match filtering, shown at the same amplitude and time scales. The dashed arrows represent the projection of the open pit, while the interior plot shows the sum of the squared amplitudes for each trace. The propagation pattern is peanut-shaped, asymmetrical such that more energy is recorded in the direction of the ripple (denoted by the solid arrow). Even though less obvious, more energy is also recorded on signals in which propagation is behind the bench.

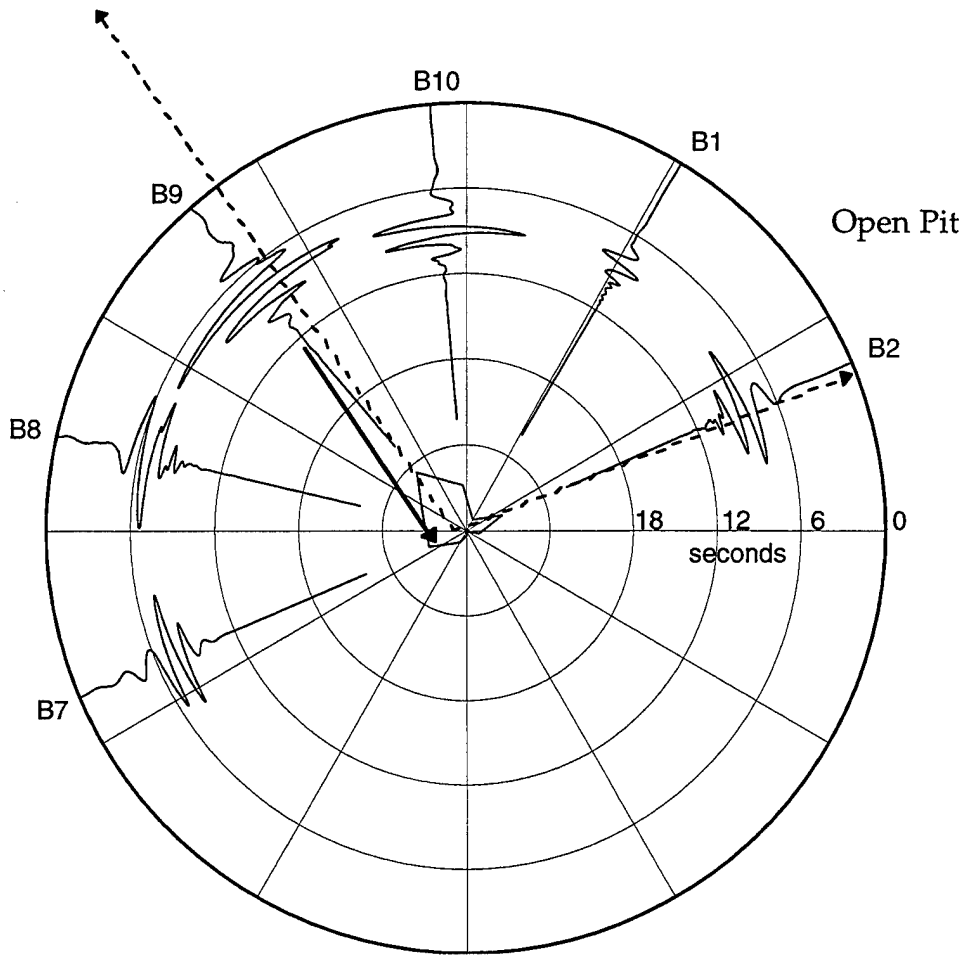

Figure A22. Azimuthal variation of Love wave energy around the Chemlime quarry for the July 12, 1994 blast. The projection of the open pit (dashed arrows) and the orientation of the ripple fire (solid arrow) are shown.

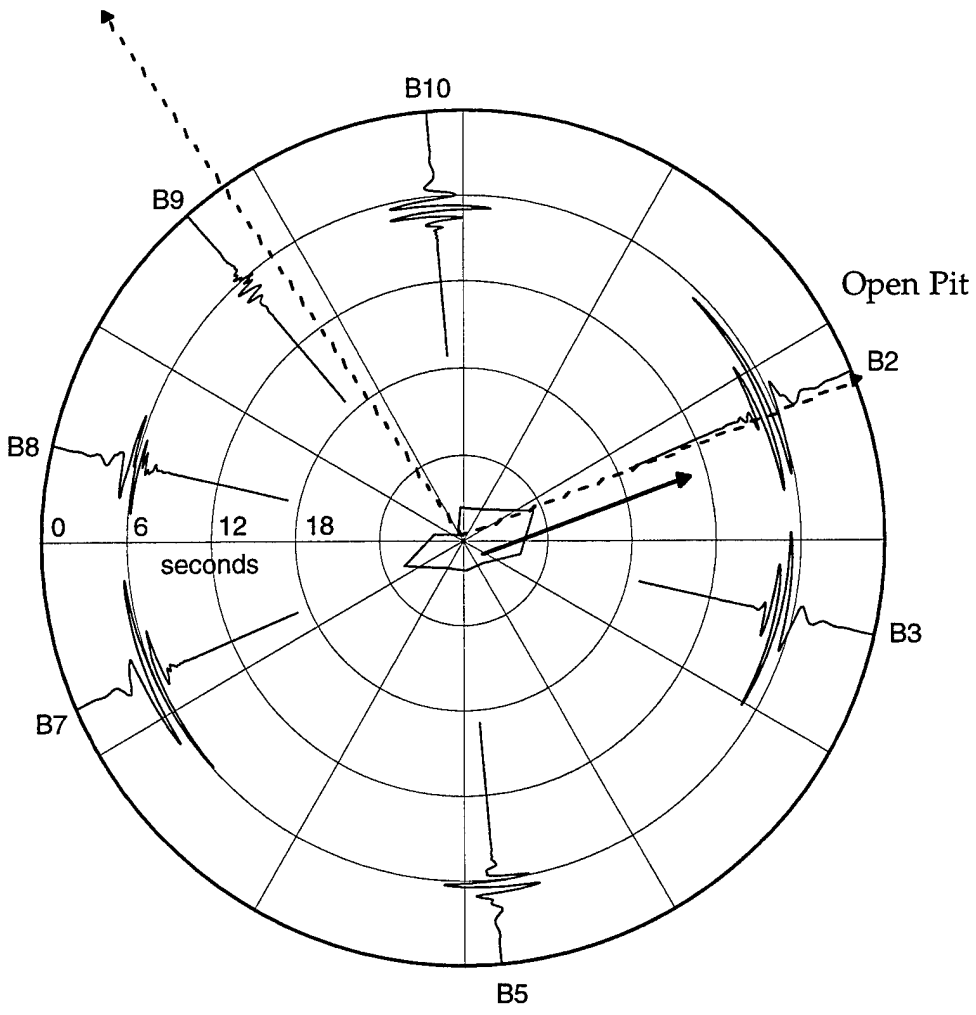

Figure A23. Azimuthal variation of Love wave energy around the Chemlime quarry for the July 17, 1994 blast. The projection of the open pit (dashed arrows) and the orientation of ripple firing (solid arrow) are shown. Changing the topographic bench caused the orientation of the long axis of the radiation pattern seen in Figures A22 and A23 to be realigned also.

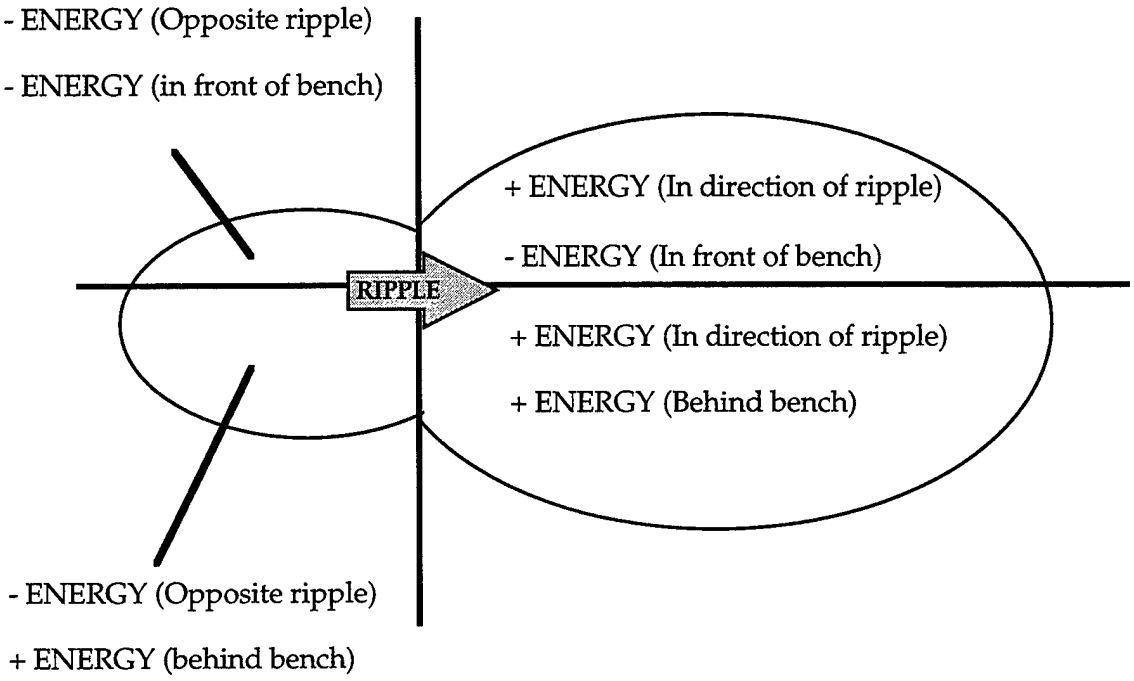

Figure A24. Proposed explanation for radiation patterns observed for Love waves in Central Texas.

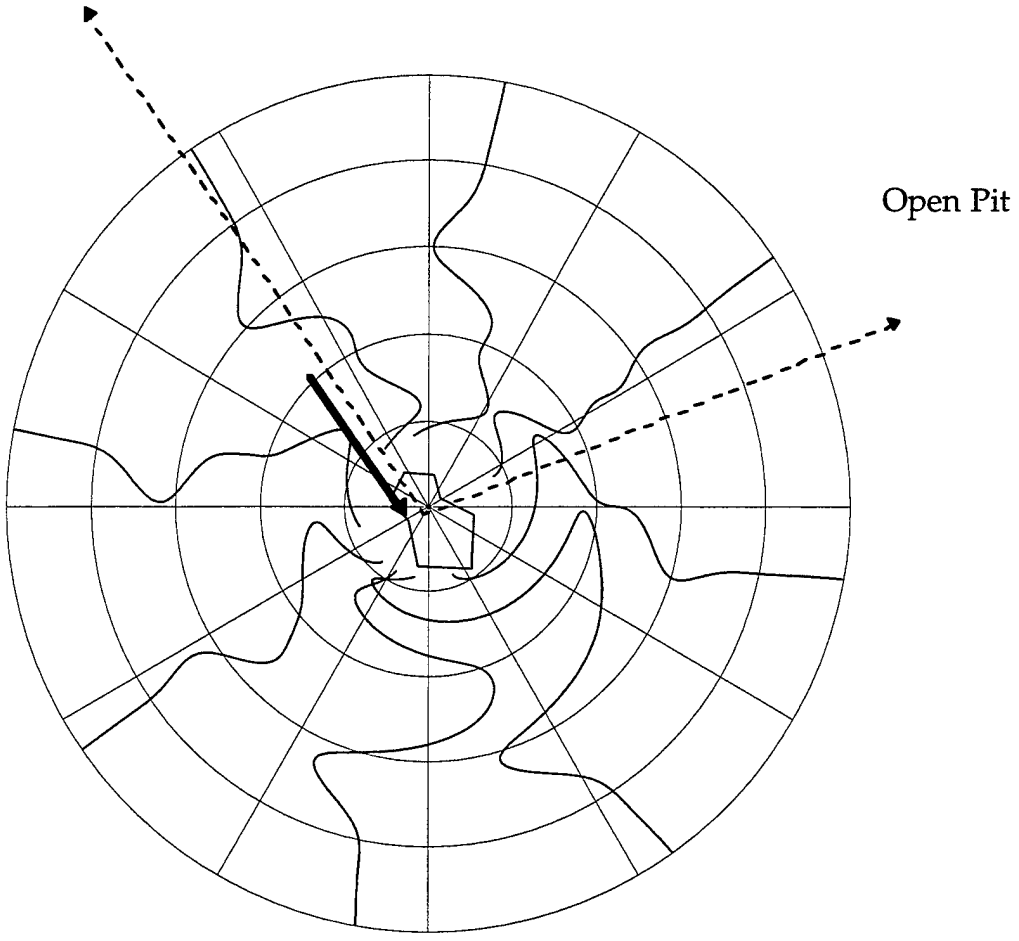

Figure A25. Finite difference seismograms (at 2 km distance) calculated from modeling the linear effect of the bench at the Chemlime quarry. The radiation pattern is consistent with that observed for Love waves.

with these observations. However, two different source mechanisms produced results similar to observed radiation patterns-- one which considers the linear effect of the bench, and the second that is a force-equivalent-spall model. Whether one or both of these models is needed to explain the source mechanisms for these quarry blasts will be determined as more detailed modeling is done.

Acknowledgments

I thank Keith McLaughlin, Eugene Herrin, and Tom Goforth for their helpful discussions and comments concerning this research. Also, Angela Maddox provided insightful comments about the manuscript, and this is greatly appreciated. Finally, without the support of Freeman Mullins and Robert "Squeaky" Shannon at Chemlime, this study would not have been completed. The work was sponsored by the Advanced Research Projects Agency, Nuclear Monitoring Office, ARPA orders A128 and C325, under Phillips Lab contracts F19628-93-C-0057 and F19628-95-C-0184.

References

Bonner, J., Herrin, E., and Goforth, T., (1996). Azimuthal variation of Rg energy in Central Texas. (in press) *Seis. Res. Let.*

Bonner, J. (1993). Crustal velocity structure of Central Texas. M.S. Thesis, Baylor University, Waco, Texas, 125 pp.

Delitsyne, L., Meyer, R., and Burkholder, P., (1996). Generation of shear waves at quarries from near-regional data (abstract). *Seis. Res. Let.*, **67**, no. 2, 29.

Dziewonski, A., Bloch, S., and Landisman, M. (1969). A technique for the analysis of transient seismic signals, *Bull. Seis. Soc. Am.* **59**, 427-444.

Goforth, T. and Herrin, E. (1979). Phase-matched filters: application to the study of Love waves, *Bull. Seis. Soc. Am.* **69**, 27-44.

Goforth, T. and Bonner, J. (1995). Characteristics of Rg waves recorded in Central Texas, *Bull. Seis. Soc. Am.* **85**, 1232-1245.

Herrin, E. and Goforth, T. (1977). Phase-matched filters: application to the study of Rayleigh waves, *Bull. Seis. Soc. Am.* **67**, 399-407.

Herrmann, R. B. (1973).Some aspects of band-pass filtering of surface waves, *Bull. Seis. Soc. Am.* **69**, 399-407.

Kafka, A. (1990). Rg as depth discriminant for earthquakes and explosions: a case study in New England, *Bull. Seis. Soc. Am*, **80**, 373-394.

McLaughlin, K. and Bonner, J. (1996). Seismic source mechanism of quarry blasts and observed Rayleigh and Love wave radiation patterns from a Texas quarry (abstract), *Seis. Res. Let.*, **67**, no. 2, 29.

Trygvasson, E. and Qualls, B. (1967). Seismic refraction measurements of crustal structure in Oklahoma, *J. Geophys. Res.* **72**. 3738-3740.

APPENDIX B-- A PRELIMINARY INVESTIGATION OF THE USE OF ACOUSTIC AND SEISMO-ACOUSTIC OBSERVATIONS TO IDENTIFY VENTED EXPLOSIVE SEISMIC SOURCES

by

G. G. Sorrells and Eugene Herrin

Introduction

Current plans for the verification of a Comprehensive Test Ban Treaty call for the collocation of infrasonic and seismic monitoring systems at future IMS sites, While the collocation strategy has been proposed primarily for logistical purposes , it may yield technical benefits as well. Vented explosions such as quarry blasts, mining shots and other types of industrial explosions can account for a significant fraction of the low magnitude, near regional seismic activity observed in many locations. Consequently, positive identification of these sources could eliminate a large number of events from further consideration as possible underground nuclear explosions. In contrast to earthquakes and fully contained explosions, vented explosions will generate acoustic as well as seismic signals. Therefore, by using data from both the seismic and infrasonic systems at the IMS sites it may be possible to distinguish vented explosions from other seismic source types. The success of this approach will be determined by the capabilities of the available monitoring systems to detect the associated acoustic signal. The pressure amplitudes of these signals are expected to peak at frequencies greater than 1 hertz and to be of the order of a few μbars or less at near regional distances from the source. Pressure transducers with system noise levels of a few tens of nanobars are commercially available at a reasonable price and have the potential to detect very weak infrasonic signals. However, this potential is rarely realizable without spatial filtering because the wind generated perturbations of the local atmospheric pressure field may be of the order of a few tens of μbars. Pipe arrays (Daniels,1959, Grover,1971) are usually coupled to the pressure transducers to provide the spatial filtering necessary to that partially suppresses the wind generated noise. A well designed pipe array may reduce wind noise by as much as 20-40 db. Nevertheless, a large fraction of the wind noise may still be passed by the pipe array during periods of moderate to high surface wind speeds because the pressure amplitudes of the

wind generated noise tend to scale as the cube of the mean wind speed (Bedard et al, 1992). This latter point is illustrated by the results shown in Figure B1. The data shown in this figure are power spectral density estimates of infrasonic noise observed at the output of a pressure transducer coupled to a conventional short period pipe array. They are representative of calm and windy intervals at the TX01 site in the TXAR seismic array. Notice that despite the use of a pipe array the infrasonic background noise levels increase by as much as 40 db as the local micrometeorological state changes from calm to windy conditions. Thus, there is a clear need to identify and investigate alternative short period infrasonic signal detection systems which may be used to supplement pressure transducer/pipe array systems during adverse wind conditions.

Donn et al (1971) proposed the use of shallow buried short period vertical seismographs to obtain improved acoustic signal to noise ratios relative to those provided by conventional infrasonic monitoring systems during periods of moderate to high surface wind speeds. Their proposal was motivated by the simultaneous observation of infrasonic signals and large acoustically coupled Rayleigh waves following the Apollo 13 and 14 launches at Cape Kennedy and by the fact that wind-generated seismic noise can be strongly attenuated by placing the seismic observation point at moderately shallow depths. Since the observation of acoustically coupled Rayliegh waves will be confined to media whose seismic wave velocities are comparable to the local sound speed (Press and Ewing, 1951), they are not likely to be observed at future IMS sites. However, Sorrells (1971) has shown that infrasonic signals also generate acoustically coupled near field earth movements which are common to all geologic environments. In this document and in future reports, the acoustically coupled near field earth motion will be referred to as the "seismo-acoustic" signal. It may be deduced from Eq (24) of this reference that for acoustic wavelengths which are much larger than the seismic observation depth but much less than the thickness of the formation containing the observation point, the amplitude of the vertical velocity component of the seismo-acoustic signal should scale linearly with the pressure amplitude of the acoustic wave and that the scaling factor should be proportional to the product of the local sound speed and the formation compressibility. The formation compressibilities at seismically

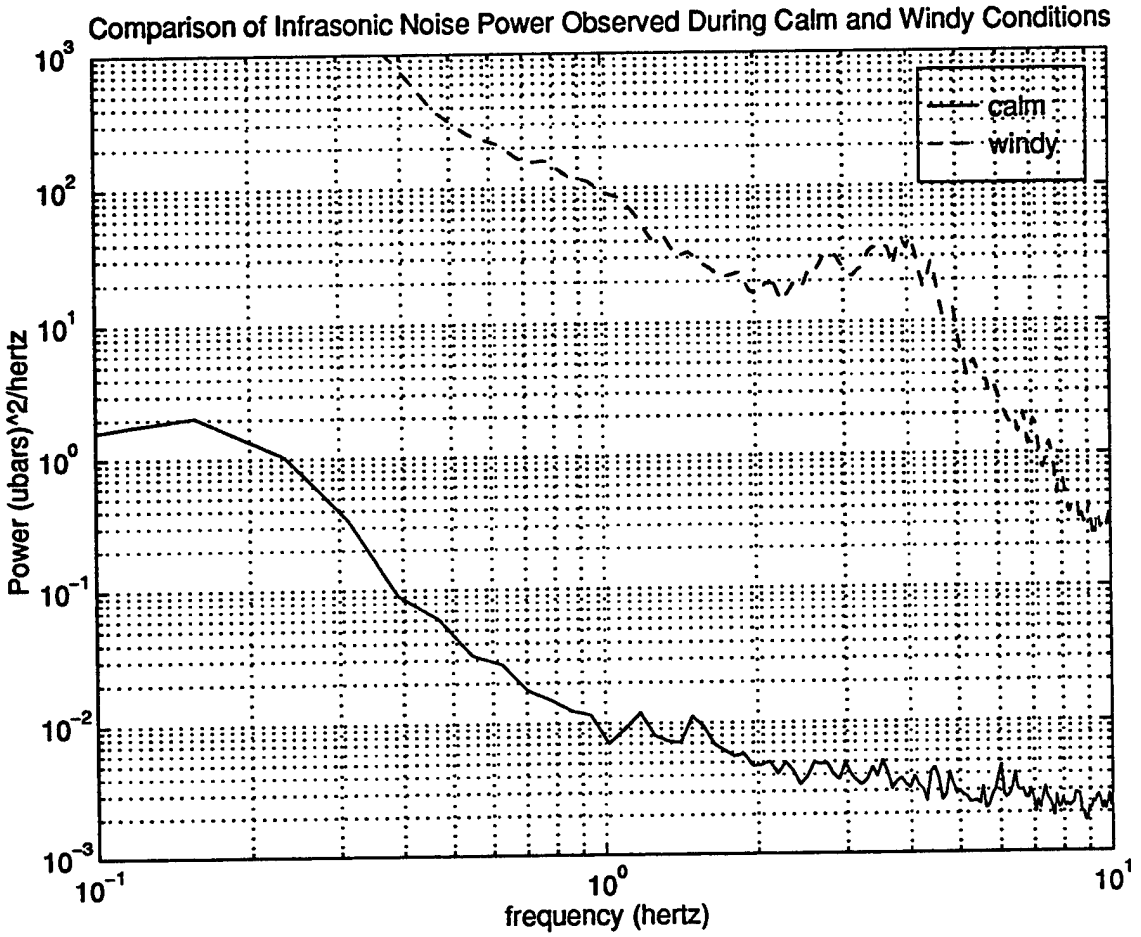

Figure B1. Power spectral density estimates of infrasonic background noise during calm and windy conditions.

"quiet" sites are expected to be of the order of 10^{-11} μbars while the local sound speed is expected to about 340-350 m/sec. Therefore, an acoustic signal with a one μbar pressure amplitude is predicted to generate a seismo-acoustic vertical velocity signal with an amplitude of about 3 nm/sec. at these types of sites. It is significant to note that the vertical component of the background noise levels at seismically "quiet" locations is typically of a similar magnitude or less at frequencies greater than about 1 hertz. For example, the rms noise threshold in the 1-4 hertz bandwidth at the TX01 site of the TXAR array during the calm and windy periods referenced above were found to be 1.5 and 2.9 nm/sec,respectively. Thus, on the basis of these arguments it may be inferred that acoustic signals with pressure amplitudes as low as one μbar at frequencies greater than 1 hertz will generate seismo-acoustic signals that may be detectable at seismically "quiet" sites during both calm and windy local atmospheric conditions. Therefore, it should be possible to use seismo-acoustic observations to supplement infrasonic observations during adverse wind conditions to aid in the detection of short-period acoustic waves at future IMS sites. Studies to investigate this possibility and to evaluate the use of acoustic data to identify near regional vented explosions were initiated in the spring of 1995. The preliminary results of these studies are briefly summarized in the following paragraphs.

Seismic Detection of Acoustic Waves

Seismo-Acoustic Transfer Functions

Suppose that a vertical seismograph system is located at a depth, **z**, beneath the surface of the earth. Assume that an infrasonic sensor system is located at the surface directly above the seismic observation point. Let **P(f)** be the pressure spectrum of a plane acoustic wave referenced to the input of the infrasonic system. Let **c** be the horizontal phase velocity of the acoustic wave. Let $\mathbf{SA_3(f,z;c)}$ be the spectrum of the vertical velocity component of the associated seismo-acoustic signal referenced to the input of the seismic system. It then follows from Sorrells and Goforth (1973) that,

$$SA_3(f,z;c) = úúúçT_3(f/c,z)úçP(f) \qquad (1)$$

where T_3 is defined to be the vertical velocity component of the seismo-acoustic transfer function.

The "Thompson Hollow" Experiment. A MATLAB code has been written to calculate the seismo-acoustic transfer function for a generic earth model consisting of multiple homogeneous, isotropic, perfectly elastic, horizontal layers. An initial test of the reliability of this model to accurately predict the seismo-acoustic transfer function observed in various geologic environments was undertaken at the "Thompson Hollow" site in central Texas. This site is located 9.75 km. west of the Chemical Lime Quarry in an area characterized by low topographic relief and "layer cake" stratigraphy. Blasts at the quarry typically occur on a semiweekly basis and thus it provides a convenient source of short period acoustic waves. An infrasonic sensor system and a short period vertical seismograph system were temporarily collocated at Thompson Hollow to record the acoustic and seismo-acoustic signals generated by blasts at the nearby quarry. The essential results of this experiment are summarized in Figures B2 and B3. The filtered waveform of an acoustic signal generated by a blast at the quarry is shown in the lower panel of Figure B2. The associated seismo-acoustic waveform is shown in the upper panel. It is important to observe that there is a phase difference of about 90° between the two waveforms. This difference can be fully explained by noting that the output of the seismograph system is proportional to particle velocity, while the output of the infrasonic system is proportional to pressure. It also implies that the "Thompson Hollow" seismo-acoustic response is to a first order, at least, perfectly elastic and that the acoustic pressures are acting on a surface that is approximately horizontal. The shallow seismic velocity structure beneath the site is approximated by the earth model shown in Figure B3a The modulus of the associated seismo-acoustic transfer function for a zero observation depth and a nominal sound speed of 0.344 km/sec is shown in Figure B3b. The observed values of the transfer function in one octave bandwidths extending from one to eight hertz are also plotted as open circles in this figure. The relatively good agreement between the observed and predicted values of the seismo-acoustic transfer function indicates that a horizontally layered earth model with the properties shown in Figure B3a is a good approximation to the shallow seismic velocity

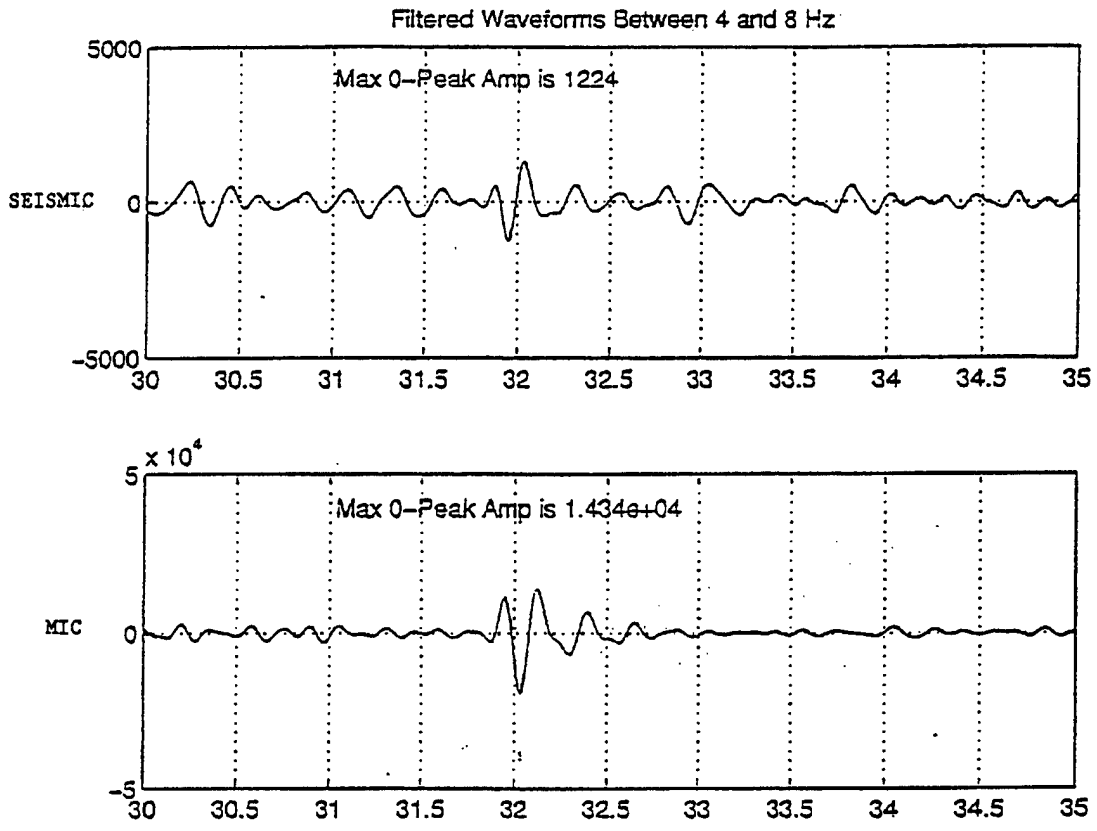

Figure B2. Filtered waveforms between 2 and 4 Hz. The lower panel shows the filtered waveform of an acoustic signal generated by a quarry blast. The upper panel shows the associated seismo-acoustic waveform.

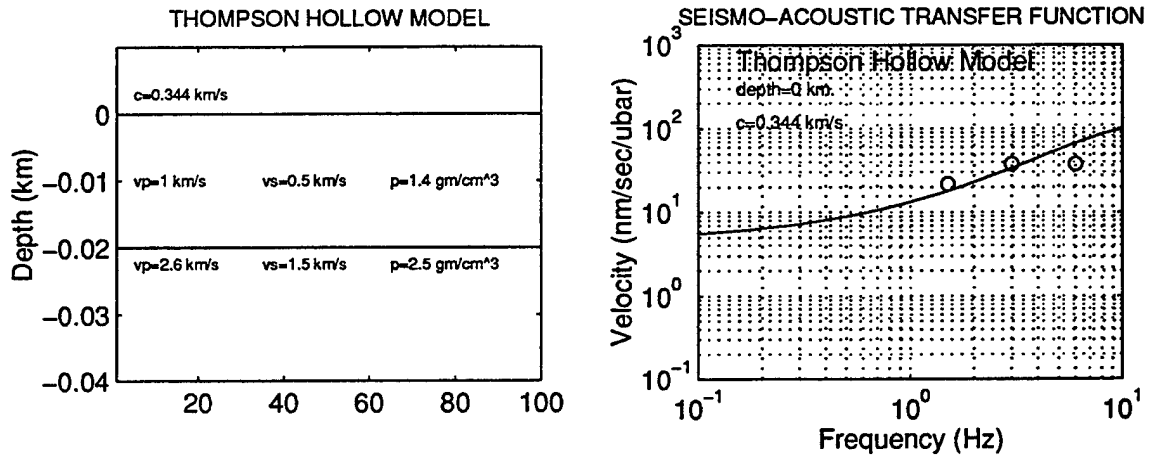

Figure B3a. Thompson Hollow model of shallow seismic velocity structure.
Figure B3b. Seismo-acoustic transfer functions.

and density structure beneath the observation point. In summary, the results of the "Thompson Hollow" experiment demonstrated that the existing model can be used with confidence to predict seismo-acoustic transfer functions in areas characterized by low topographic relief and "layer cake" stratigraphy.

The TXAR Experiments. In the fall of 1995, a short period infrasonic sensor system was collocated with the TX01 short period vertical seismograph system in the TXAR array. The purpose of this installation was to acquire acoustic data to aid in the confirmation of apparent seismo-acoustic detections that had been previously reported at TXAR. It also provided the opportunity to test the reliability of the existing model to accurately predict the seismo-acoustic transfer function observed in a geologic environment that is significantly different from the "Thompson Hollow" site.

An example of an acoustic signal and its associated seismo-acoustic signal as recorded by the TXAR array is shown in the upper panel of Figure 4 In this figure, the seismic channels are identified by the **sz** prefix while the infrasonic channel is identified by the **aa** prefix. These data were recorded during a period of light surface winds at TXAR. The seismo-acoustic signal is partially obscured by the coda of a prior near regional event but a prominent acoustic signal is observed on the infrasonic channel. The seismic records of the seismo-acoustic signal are time aligned in the lower panel of Figure B4. The time shifts required to achieve this alignment were determined by passing the seismic channels through a matched filter whose impulse response was the time reverse of the acoustic signal then noting the arrival time of the maximum filter output. Analysis of the time shift data indicated that the horizontal phase velocity of the signal is 0.352 km/sec and that its azimuth is 294.° The beam formed by summing the time aligned seismic channels is shown on the **beam2** channel. Notice that simple beamforming has resulted in a significant improvement in the seismo-acoustic signal to noise ratio. This result is surprising since the TXAR sensor spacing is large compared to acoustic wavelengths at frequencies greater than 1 hertz. It is also important to observe that the beamed seismo-acoustic waveform essentially replicates the acoustic waveform for at least 5 seconds. This result implies the absence of significant acoustic multi-pathing effects over the dimensions of the array.

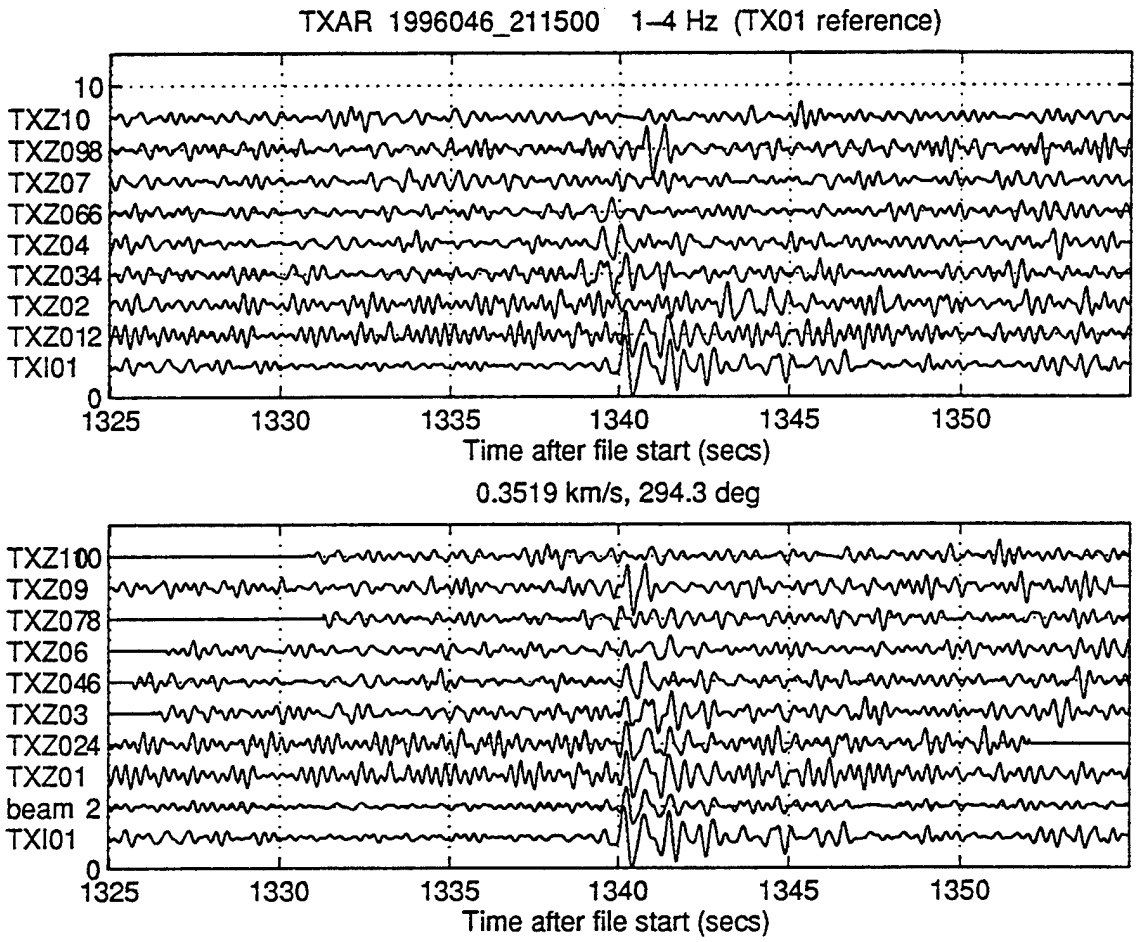

Figure B4. TXAR traces and beamformed traces. Upper panel shows acoustic signal (Channel aa01) and the seismo-acoustic signals on the other channels. Lower panel shows the alined seismic records of the seismo-acoustic signal.

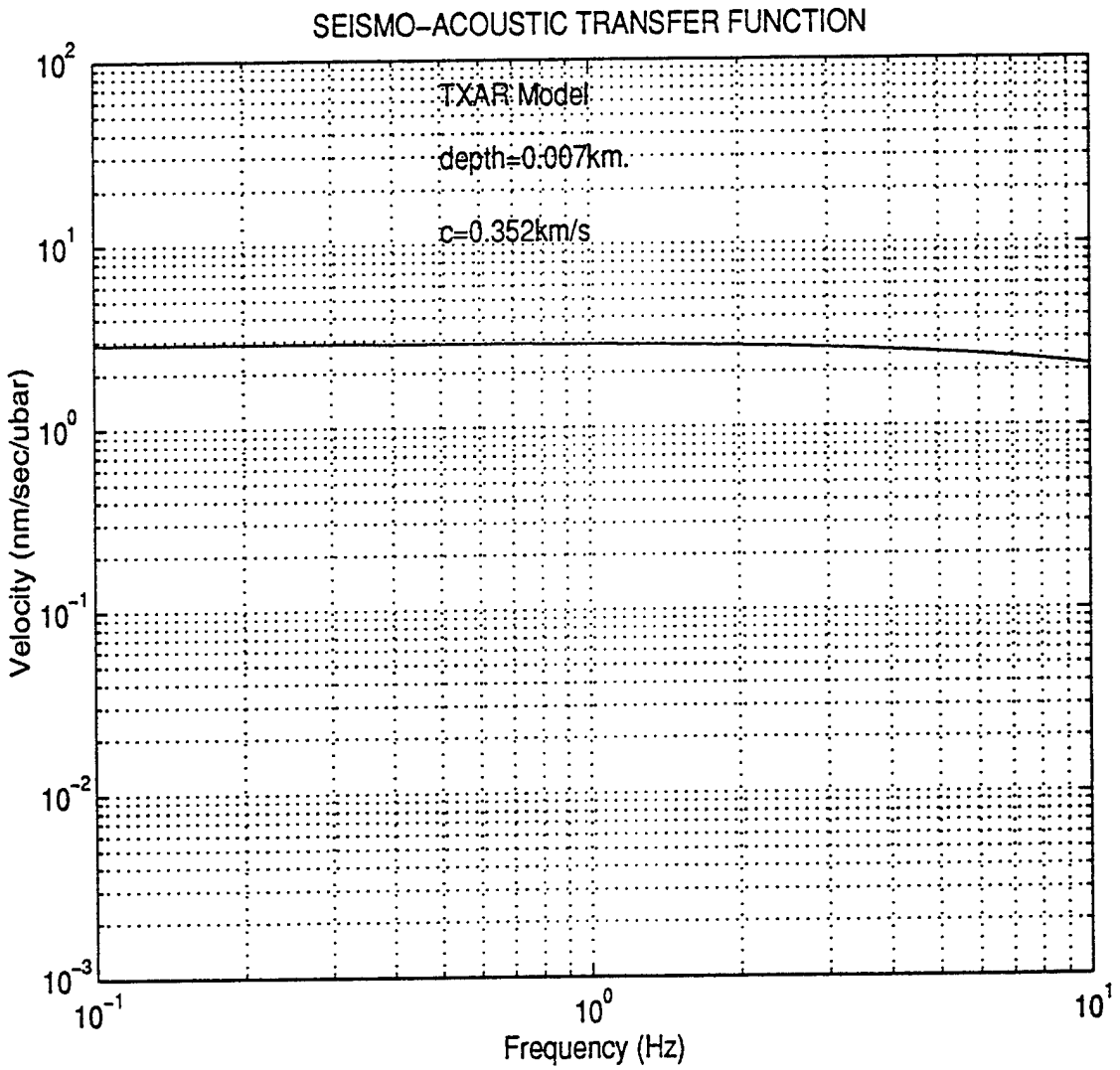

Figure B5. Seismo-acoustic transfer functions for TXAR model.

It also indicates that the TXAR seismo-acoustic transfer functions are sensibly constant in the 1-4 hertz band width. As shown in Figure B5, this result is consistent with predictions. The solid curve plotted in this figure is the modulus of the predicted TXAR seismo-acoustic transfer function for a sound speed of 0.352 km/sec and a nominal seismic observation depth of 0.007 km. Notice that at frequencies less than about 10 hertz, it asymptotically approaches a value of about 3 nm/sec/μbar. Therefore, at frequencies less than 10 hertz, the seismo-acoustic signal is expected be a scaled replica of the acoustic signal with a scaling factor of about 3 nm/sec/μbar. While the experimental data validates the prediction of a shared common waveform, the experimental results shown in Figure B6 indicates that the model significantly overestimates the observed seismo-acoustic scaling factor. The acoustic and seismo-acoustic waveforms detected in the 1-4 hertz bandwidth at TX01 are shown individually in the upper and middle panels of Figure B7 and are overlain in the lower panel. To facilitate the estimation of the scaling factor, the acoustic signal waveform was filtered to match the nominal response of the short period seismograph system. It can be seen from this comparison that a generous estimate of the observed scale factor is about 0.7 nm/sec/μbar or about 10-12 db less than the predicted value. The model of the shallow TXAR earth structure used for the calculation of the seismo-acoustic transfer function is shown in Figure 8. It is based upon the results of a shallow seismic refraction survey carried out in the immediate vicinity of TX01 and reported by Sandige-Bodoh (1989). In order to account for the discrepancy between the observed and predicted scaling factors the seismic velocities determined by this survey would have to been underestimated by as much as a factor of 2. The occurrence of a systematic error of this magnitude is extremely doubtful. It seems more likely that the discrepancy between the observed and predicted scaling factors indicates the existence of fundamental differences between the elastic properties of shallow TXAR earth structure and those characterizing the generic model currently used for the prediction of seismo-acoustic transfer functions. In this regard, it may be significant to note that the shallow structure at TXAR is characterized by pervasive vertical fracture sets that are dry to depths on the order on the order of 1,000 feet. This phenomenon may result in an anisotropic elastic response to surface applied pressure changes which is not accounted for by the existing model. Nevertheless, the results of the TXAR experiments have

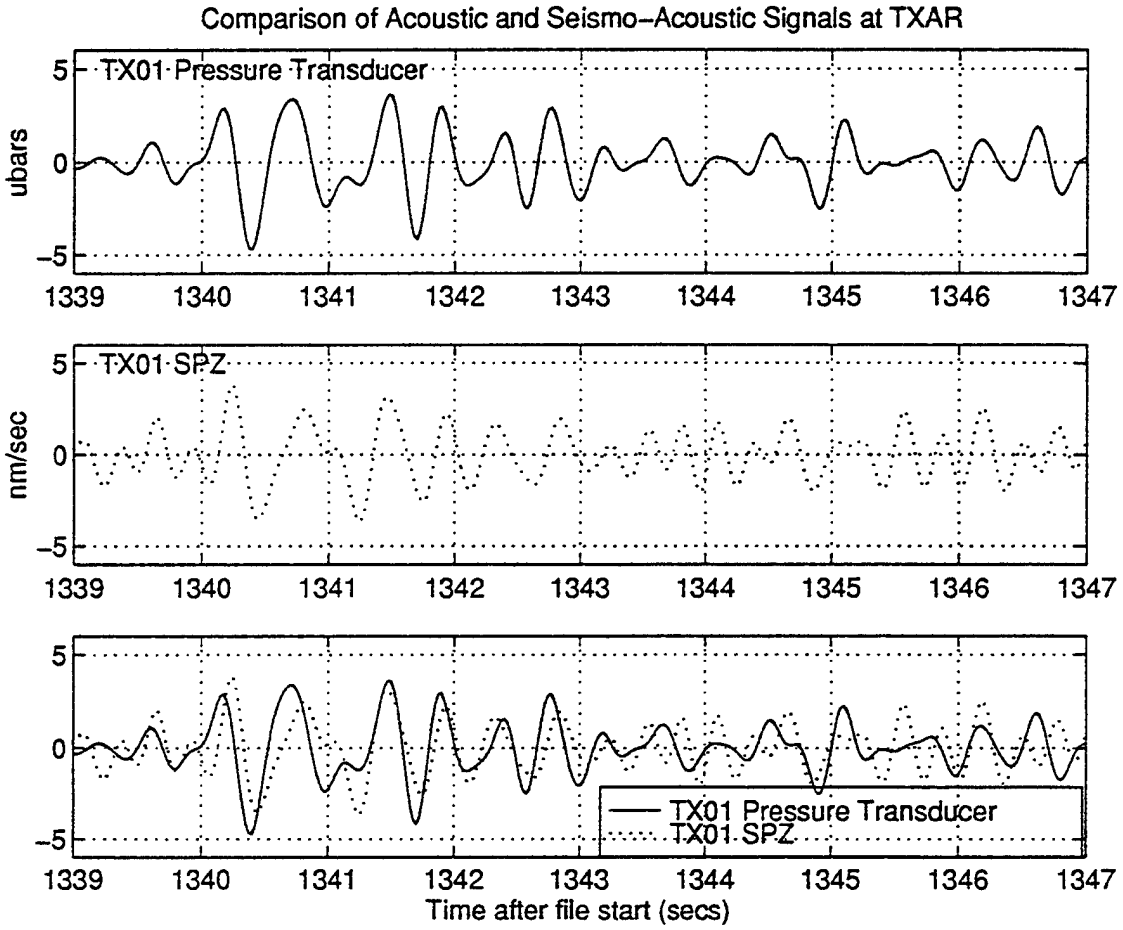

Figure B6. Comparison of acoustic and seismo-acoustic signals at TXAR. The acoustic and seismo-acoustic signals are shown individually in the upper and middle panels. The two signals are overlain in the lower panel.

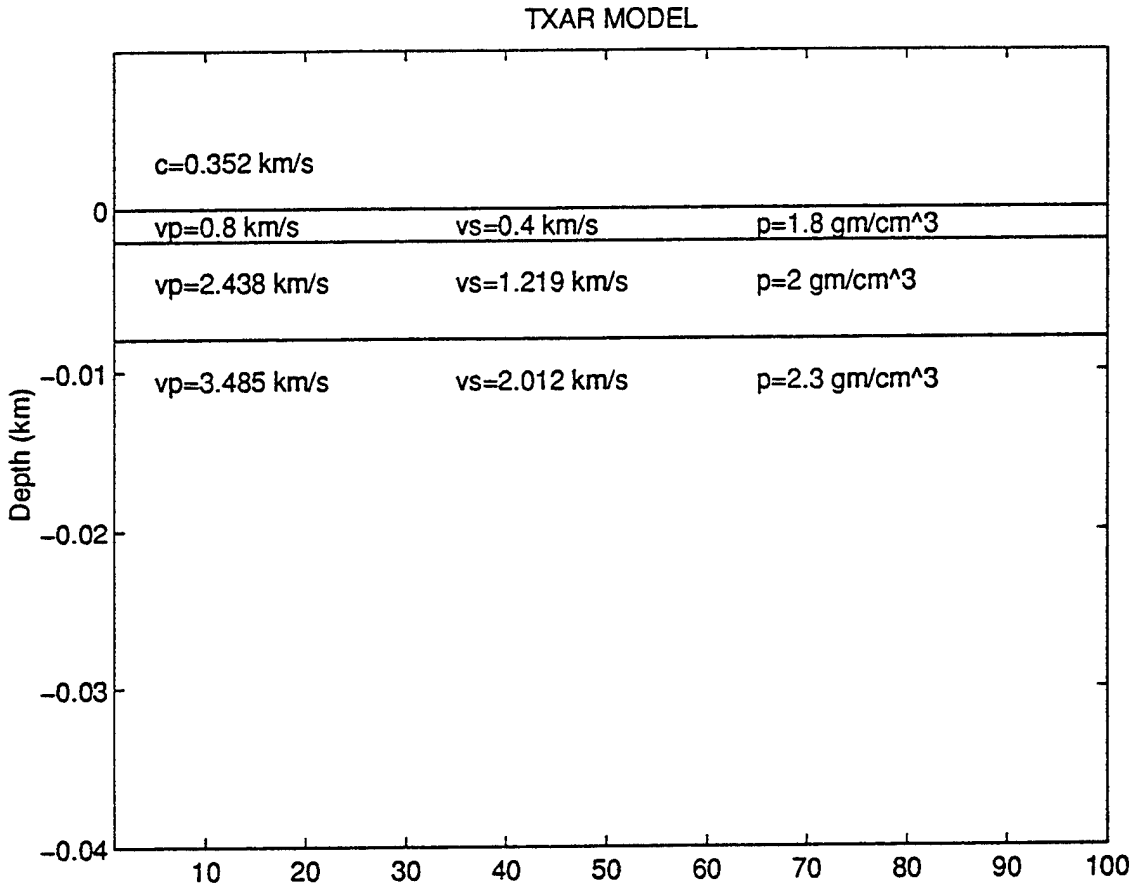

Figure B7. Model of shallow earth structure at TXAR.

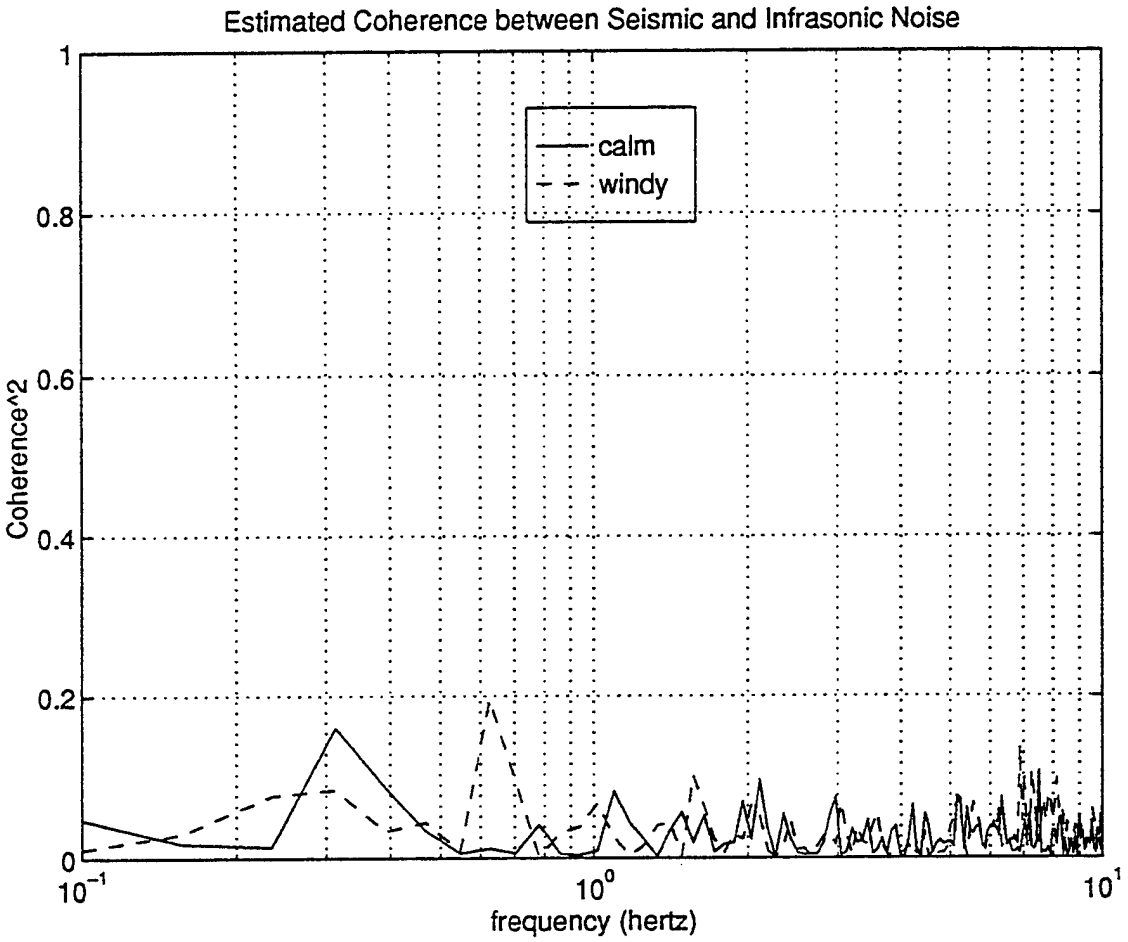

Figure B8. Estimated coherence between infrasonic and seismic data during calm and windy periods.

thus far demonstrated that acoustic signals with amplitudes of a few μbars at frequencies greater than 1 hertz generate seismo-acoustic signals that are detectable at a "quiet" seismic site despite the discrepancy between observed and predicted scaling factors.

Seismo-Acoustic Correlation Detection of Short Period Acoustic Signals at TXAR

The results presented in the previous section demonstrate that short period acoustic and seismo-acoustic signals share a common waveform at TXAR. Furthermore, as indicated by the coherence estimates shown in Figure B8, short period seismic and infrasonic noise at frequencies greater than 1 hertz may be considered to be statistically independent processes under both calm and windy atmospheric conditions. Therefore, a running estimate of the normalized correlation coefficient for simultaneously acquired seismic and infrasonic data sets from collocated sensors should provide a simple and effective method for the detection of short period acoustic signals at TXAR.

A MATLAB code has been written to estimate the normalized correlation coefficient between two input data records. In its current configuration, the code accepts records of selectable lengths from the outputs of the collocated TX01 short-period vertical seismograph and pressure transducer. The records are filtered to account for differences in nominal sensor system responses and to pass data in the 2-8 hertz bandwidth. Estimates of the normalized correlation coefficient are currently made in a 5 second window which is sequentially shifted forward in one second intervals. The output of the code is a time series whose amplitudes are found in the interval **[-1,1]** and whose sample points are separated by 1 second in input record time. The values of this time series are expected to cluster near zero when both data records contain noise only and to be greater than zero when the records contain acoustic and seismo-acoustic signals plus noise. This configuration has been tested by using pairs of synthetically generated, statistically independent, normally distributed data records. The objective of the test was to estimate "false alarm" probability distribution characterizing this particular correlator code configuration.. The histogram showing the frequency of occurrence distribution for the synthetic sample correlation coefficients is shown in

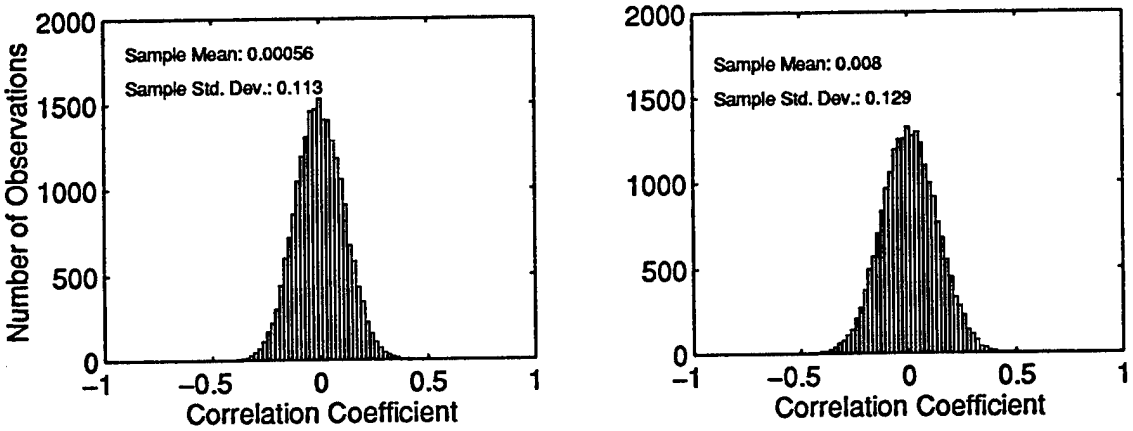

Figure B9a. Correlation code test results with synthetic Data
Figure B9b. Correlation test results with real data.

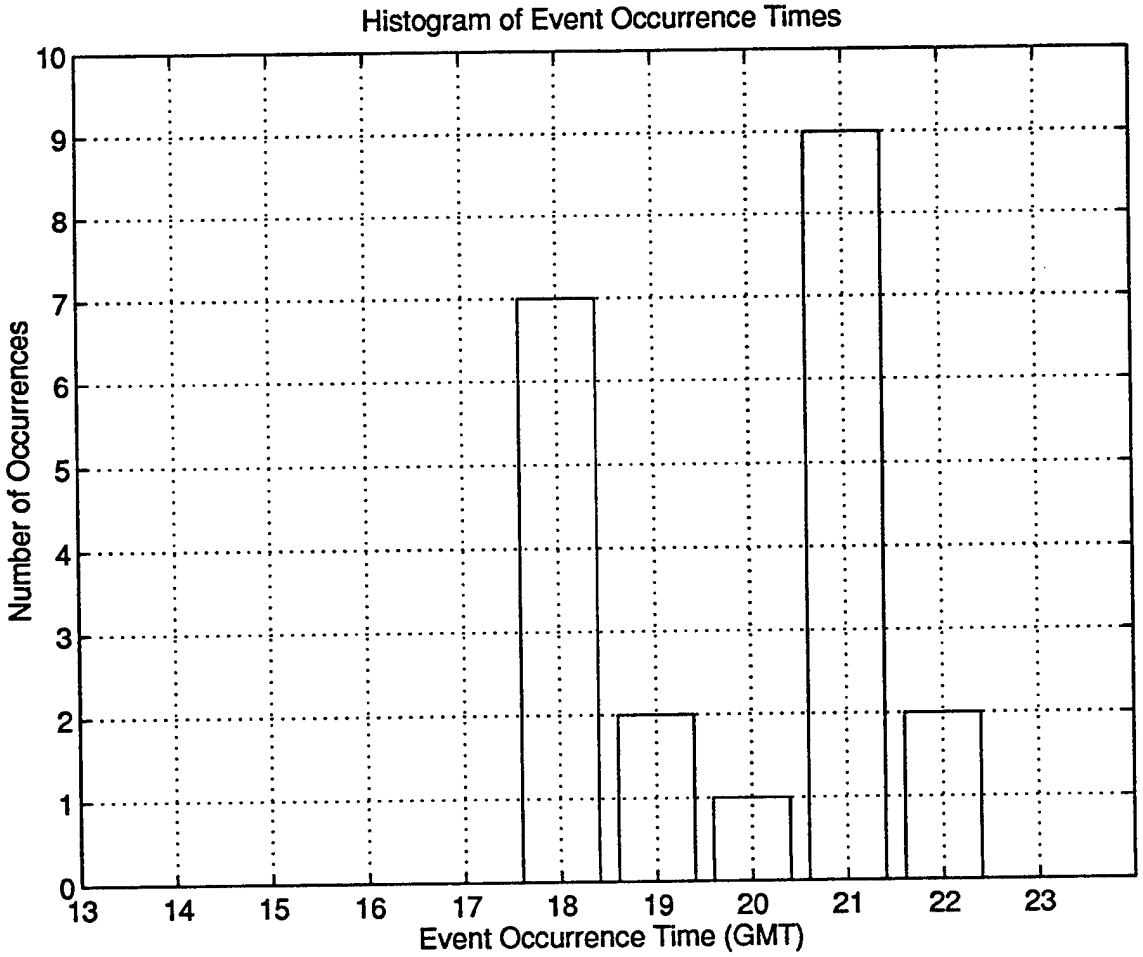

Figure B10. Histogram of occurrence times of seismic events

Figure B9a. Notice that the sample population is normally distributed with a near zero mean and a standard deviation of 0.112. An identical test was performed on real data acquired during intervals that were free of visible seismic signals. The resulting histogram showing the frequency of occurrence distribution for the real sample correlation coefficients is shown in Figure B9b. Observe that this sample population appears to be normally distributed with a slightly positive mean. It should also be noted that the standard deviation of the sample population drawn from the real data sets is somewhat larger than the standard deviation characterizing the synthetic population. These differences are believed to indicate that naturally occurring acoustic events make a minor but statistically significant contribution to the seismic and acoustic data recorded in the 2-8 hertz passband at TXAR.

Seismo-Acoustic Identification of Vented Near Regional Explosions

It was argued in the introduction to this text that the detection of an acoustic signal and its association with a prior seismic event unambiguously identifies the source of both as a vented explosion. A preliminary test was undertaken to determine if this approach could be successfully applied to the identification of vented explosions in a limited sample of the population of near regional seismic events detected at TXAR. The test was conducted during a 7 week interval extending from 7 November 1995 to 10 January 1996. During this time period, 25 work-day records of the seismic data acquired at TXAR during local daylight hours (1300-2300 GMT) were reviewed to identify the arrival times of all potentially locatable near regional seismic events. The seismo-acoustic correlator code, operating in the configuration referenced above, was used to detect acoustic events. It was applied to the outputs of the collocated seismic and infrasonic sensors at TX01 in a 45 minute time period which included the arrival time of the seismic event plus at least 25 minutes for each identified event. The correlator code detection threshold was set at 0.3. Based upon the test results identified in the previous section, the corresponding probability of a false alarm is expected to be less than 0.005. If the correlator code output was found to be equal to or in excess of 0.3 at any time in a 20 minute window starting 5 minutes after the p arrival time, a possible associated acoustic event detection was declared and the seismic array

data was analyzed to estimate the distance and azimuth to the epicenter of the seismic event and its approximate origin time. The apparent group velocity of each acoustic event detection, referenced to the epicenter and origin time of the seismic event was then determined. If the apparent group velocity of any one of the acoustic event detections was found to lie in the interval from 0.27 km/sec to 0.33 km/sec it was assumed to be associated with the seismic event and thus identifies the source of both as a probable vented explosion. During the 25 day test period the sources of 21 near regional seismic events were identified as probable vented explosions by the application of the procedures outlined above. A histogram of the occurrence times of these events is shown in Figure B10. Notice that their occurrence times tightly cluster near 1800 and 2100 hours (noon and 3 PM, local time). This observation strongly implies that the events are the result of industrial processes and is consistent with the identification of their sources as vented explosions. The approximate locations of their estimated epicenters are shown in Figure B11. These locations were derived from azimuth and distance estimates calculated from the array data for each event. The azimuth from TXAR to the epicenters were estimated from the p arrival time data The following equation was used to estimate the approximate epicentral distance

$$D(km)=6.22(dT + 6.5) \qquad (2)$$

where **dT** is the observed difference in the p and Lg arrival times. This equation has been found to yield reliable estimates of distances to the known epicenters of selected near regional events north and northwest of TXAR. The hachured area in Figure B11 identifies a coal mining district in northern Mexico which is thought to be a likely source of the majority of near regional events located east southeast of TXAR. If it is, then the epicentral data indicate that Eq (2) significantly overestimates epicentral distances for near regional sources east of the array. In this regard, it was also found that the acoustic arrivals detected by the correlator code were systematically early when referenced to the estimated epicenters east and south of the array. Thus, pending the results of calibration studies now underway at TXAR, it is tentatively concluded that:

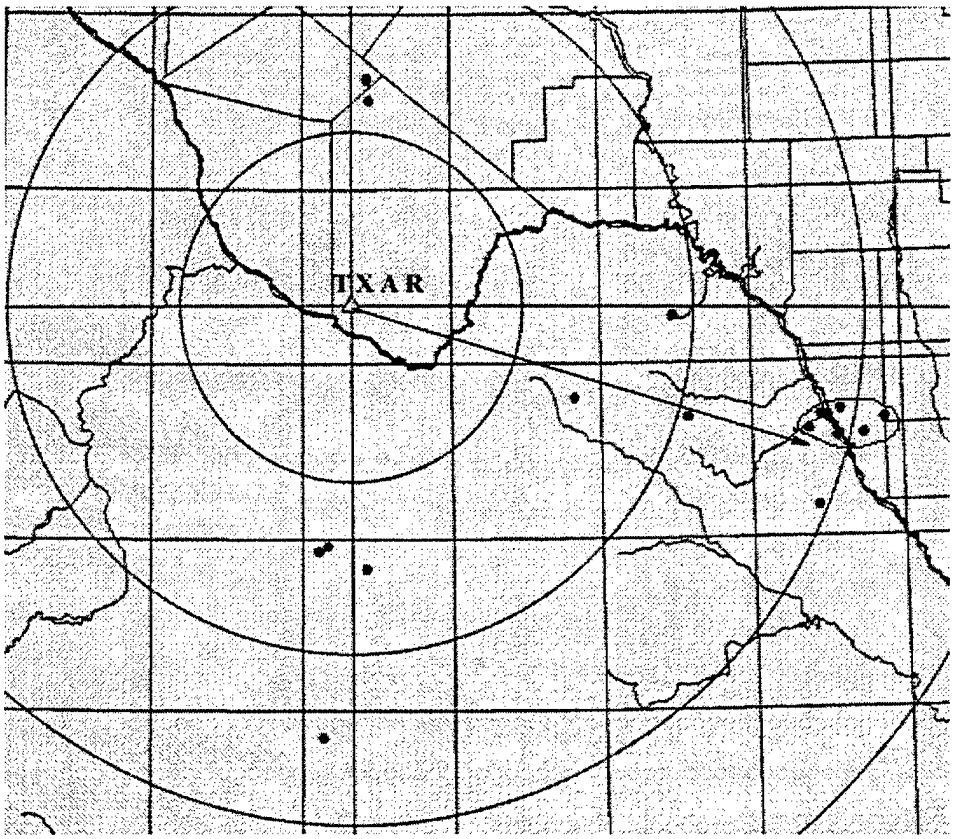

Figure B11. Location map of acoustical events recorded at TXAR.

1. At least some of the events identified as vented explosions during this test were generated in the northern Mexico coal mining district identified in Figure B11 and,

2. The use of the correlator code provides a simple but effective method for the detection of the relatively weak acoustic signals generated by near regional vented explosions.

Summary and Conclusions

The results presented above demonstrate that short period acoustic signals with pressure amplitudes of a few μbars or less will generate seismo-acoustic signals that are detectable at a seismically "quiet" site. This observation implies that they will also be detectable at future IMS sites which are most likely to be located in quiet seismic environments. While the short period acoustic SNR will be higher at the outputs of the infrasonic monitoring system during periods of calm to light surface winds, it may be inferred from the results shown in Figures B1 and B4 that the seismo-acoustic SNR will be higher during periods of moderate to high surface winds. The results shown in Figure B4 also indicate that seismic beamforming may significantly enhance seismo-acoustic SNR's despite the fact that the seismic array is not optimally configured for short period acoustic observations. This result is attributed to the fact that unlike seismic signals, seismo-acoustic signals are not significantly affected by multi-pathing and remain spatially stable over the characteristic dimensions of a typical IMS seismic array. Thus, it may be inferred that the seismic monitoring systems installed at future IMS sites may be used as a backup infrasonic system during those periods when local atmospheric turbulence impairs the detection capability of the primary acoustic monitoring system.

The preliminary results of this study also demonstrate that the calculation of a running estimate of the normalized correlation coefficient between the outputs of collocated seismic and infrasonic sensors provides a simple but effective method for the detection of weak short period acoustic waves. The success of this approach at TXAR is attributed to the fact that while short period acoustic and seismo-acoustic signals share a common waveform, short period seismic and infrasonic noise are, for all practical purposes, statistically

uncorrelated under both calm and windy atmospheric conditions. Statistically uncorrelated short period seismic and infrasonic noise is expected to be a property of all "hard rock" geologic environments including those which are likely to be the sites of future IMS installations. However, while acoustic and seismo-acoustic signals are always linearly related, they will share a common waveform only in those environments where the seismic velocities of the formation containing the seismic observation point are uniform over a depth range that is large compared to the wavelengths of the acoustic signals. In other environments, it will be necessary to determine the frequency response characteristics of the seismo-acoustic transfer function in order to optimize the performance of the correlator code. In this regard, it has been shown that the existing model for the prediction of seismo-acoustic transfer functions suffered from serious defects when it was tested at TXAR. Until the discrepancies between the observed and predicted values of the seismo-acoustic scaling factors at TXAR can be explained, experimental measurements should be used to determine the frequency response characteristics of local seismo-acoustic transfer functions.

Finally, the results of this study infer that the detection of a short period acoustic signal and its association with an antecedent near regional seismic event is a promising method for the identification of vented explosive sources. If further research confirms this premise then it follows that the data that will be provided by the collocated seismic and infrasonic monitoring systems at future IMS sites may be used to significant advantage to eliminate the seismic signals generated by vented explosions from further consideration as possible indicators of a clandestine underground nuclear explosion.

Acknowledgments

The authors would like to acknowledge the contributions of Jack Swanson who provided much of the data processing results summarized in this paper and who first demonstrated the advantages of seismo-acoustic beam forming. In addition, the experimental results presented in this paper are the result of detailed field work and could not have been acquired without the careful efforts of Paul Golden, Karl Thomason and Chris Hayward.

References

Bedard, A.J., R.W. Whittaker, G.E. Greene, P. Mutschlecner, R.T. Nishiyama, and M. Davidson (1992) Measurements of pressure fluctuations near the surface of the earth, Tenth Symposium on Turbulence and Diffusion 29 Sept-2 Oct 1992, Portland OR, *Am. Meteor. Soc.* 293-296

Daniels, F. B. (1959) Noise reducing line microphone for frequencies below 1c/s. *Jour. acoust. soc. Am*, **31**, 529.

Donn,W. L,,I. Dalins, V. McCarty, M. Ewing and G. Kashak (1971) Air coupled seismic waves at long range from Apollo launchings. Geophys. *Jour. R. Astrom. Soc.*, **26**, 161-171.

Grover, F. H. (1971) Experimental noise reducers for an active microbarograph array. *Geophys. Jour. R. Astrom. Soc.*, **26**, 41-52.

Press, F. and M. Ewing (1951) Ground roll coupling to atmospheric compressional waves. *Geophysics* **16**, 416-430.

Sandige-Bodah, Victoria (1989) investigating the effect fractures have on seismic wave velocities at Lajitas, Texas, seismic station: Report No. GL-TR-89-0153, Geophysics Laboratory, Hanscom AFB, MA 01731-5000. ADA215943.

Sorrells, Gordon G. (1971) A preliminary investigation into the relationship between long-period noise and local fluctuations in the atmospheric pressure field, *Geophys. Jour. R. Astrom. Soc.*, **26**, 71-82.

Sorrells, G. G. and T. T. Goforth (1973) Low-frequency earth motion generated by slowly propagating partially organized pressure fields, *Bull. Seis. Soc. Am.*, **63**, 1583-1601.

APPENDIX C – RUSSIAN MILITARY OFFICIALS VISIT SMU SEISMIC STATION DESIGNED TO DETECT UNDERGROUND NUCLEAR EXPLOSIONS

SMU News Release of 16 November 1995

Gary Shultz

SMU Office of News and Information (214) 768-7650

DALLAS (SMU) -- Military representatives of the Russian Federation today visited Southern Methodist University's Lajitas seismic station, a state-of-the-art monitoring facility which is expected to playa key role in enforcing a comprehensive test ban on nuclear tests.

The representatives -- joined by U. S. Defense Department officials -- visited the station to study its design as part of their plans for constructing similar stations in the Russian Federation. Lajitas is located in the Texas Big Bend, about 450 miles southwest of Dallas.

Representing the Russian Federation were Colonel-General Yevgeniy Petrovich Maslin, Major-General Yurie Vladimirovich Cherepanov and Colonel Vladimir Vital'evich Kovalinko. Maslin is Commander of the Federation's Special Monitoring Service and Deputy Commander of the Central Directorate of the Ministry of Defense; and Kovalinko is chief engineer and Deputy Commander of the Special Monitoring Service.

Also visiting the SMU station were representatives of the Air Force Technical Applications Center of the U. S. Department of Defense.

The station is a prototype for seismic arrays to be located worldwide as part of an international monitoring system. It was developed by Dr. Eugene Herrin, Shuler-Foscue Professor of Geological Sciences in SMU's Dedman College, with support from the Advanced Research Projects Agency of the U. S. Department of Defense.

Herrin's research team developed the station's systems and devices for detecting and reporting the detonation of underground nuclear devices anywhere in the world.

The Lajitas station, which has been in continuous operation since 1980, served as one of the U. S. monitoring stations during the first two Group of Scientific Experts Technical Tests (GSETT) in 1984 and 1990.

In 1994, the station was upgraded to a nine-element array of detection devices -- code name TXAR. It now serves as a primary station for the GSETT Third Technical Test, that began January 1, 1995.

Research and technological advances by Herrin's team now makes it possible to set up such seismic arrays almost anywhere in the world at a relatively low cost. The TXAR array uses modern seismic data acquisition equipment placed in boreholes, the Global Positioning System, radio frequency digital modems and solar power systems at each array element.

Russian Federation officials will be among representatives of 30 nations meeting at SMU Friday through Sunday to discuss arms control and treaty verification issues affecting global arms control negotiations. More than 170 participants in the annual conference will include arms control experts, policymakers, and other representatives of government agencies, industries, academic institutions and military organizations from around the world.

This year's conference, titled "Arms Control in a Multi-Polar World" is SMU's sixth in a series. It is hosted by the university's John Goodwin Tower Center for Political Studies and Dedman College.

THOMAS AHRENS
SEISMOLOGICAL LABORATORY 252-21
CALIFORNIA INSTITUTE OF TECHNOLOGY
PASADENA, CA 91125

SHELTON ALEXANDER
PENNSYLVANIA STATE UNIVERSITY
DEPARTMENT OF GEOSCIENCES
537 DEIKE BUILDING
UNIVERSITY PARK, PA 16801

RICHARD BARDZELL
ACIS
DCI/ACIS
WASHINGTON, DC 20505

DOUGLAS BAUMGARDT
ENSCO INC.
5400 PORT ROYAL ROAD
SPRINGFIELD, VA 22151

WILLIAM BENSON
NAS/COS
ROOM HA372
2001 WISCONSIN AVE. NW
WASHINGTON, DC 20007

ROBERT BLANDFORD
AFTAC
1300 N. 17TH STREET
SUITE 1450
ARLINGTON, VA 22209-2308

RHETT BUTLER
IRIS
1616 N. FORT MEYER DRIVE
SUITE 1050
ARLINGTON, VA 22209

CATHERINE DE GROOT-HEDLIN
SCRIPPS INSTITUTION OF OCEANOGRAPHY
UNIVERSITY OF CALIFORNIA, SAN DIEGO
INSTITUTE OF GEOPHYSICS AND PLANETARY PHYSICS
LA JOLLA, CA 92093

SEAN DORAN
ACIS
DCI/ACIS
WASHINGTON , DC 20505

RICHARD J. FANTEL
BUREAU OF MINES
DEPT OF INTERIOR, BLDG 20
DENVER FEDERAL CENTER
DENVER, CO 80225

RALPH ALEWINE
NTPO
1901 N. MOORE STREET, SUITE 609
ARLINGTON, VA 22209

MUAWIA BARAZANGI
INSTITUTE FOR THE STUDY OF THE CONTINENTS
3126 SNEE HALL
CORNELL UNIVERSITY
ITHACA, NY 14853

T.G. BARKER
MAXWELL TECHNOLOGIES
P.O. BOX 23558
SAN DIEGO, CA 92123

THERON J. BENNETT
MAXWELL TECHNOLOGIES
11800 SUNRISE VALLEY DRIVE SUITE 1212
RESTON, VA 22091

JONATHAN BERGER
UNIVERSITY OF CA, SAN DIEGO
SCRIPPS INSTITUTION OF OCEANOGRAPHY IGPP, 0225
9500 GILMAN DRIVE
LA JOLLA, CA 92093-0225

STEVEN BRATT
NTPO
1901 N. MOORE STREET, SUITE 609
ARLINGTON, VA 22209

LESLIE A. CASEY
DOE
1000 INDEPENDENCE AVE. SW
NN-40
WASHINGTON, DC 20585-0420

STANLEY DICKINSON
AFOSR
110 DUNCAN AVENUE, SUITE B115
BOLLING AFB
WASHINGTON, D.C. 20332-001

DIANE I. DOSER
DEPARTMENT OF GEOLOGICAL SCIENCES
THE UNIVERSITY OF TEXAS AT EL PASO
EL PASO, TX 79968

JOHN FILSON
ACIS/TMG/NTT
ROOM 6T11 NHB
WASHINGTON, DC 20505

MARK D. FISK
MISSION RESEARCH CORPORATION
735 STATE STREET
P.O. DRAWER 719
SANTA BARBARA, CA 93102-0719

LORI GRANT
MULTIMAX, INC.
311C FOREST AVE. SUITE 3
PACIFIC GROVE, CA 93950

I. N. GUPTA
MULTIMAX, INC.
1441 MCCORMICK DRIVE
LARGO, MD 20774

JAMES HAYES
NSF
4201 WILSON BLVD., ROOM 785
ARLINGTON, VA 22230

MICHAEL HEDLIN
UNIVERSITY OF CALIFORNIA, SAN DIEGO
SCRIPPS INSTITUTION OF OCEANOGRAPHY IGPP, 0225
9500 GILMAN DRIVE
LA JOLLA, CA 92093-0225

EUGENE HERRIN
SOUTHERN METHODIST UNIVERSITY
DEPARTMENT OF GEOLOGICAL SCIENCES
DALLAS, TX 75275-0395

VINDELL HSU
HQ/AFTAC/TTR
1030 S. HIGHWAY A1A
PATRICK AFB, FL 32925-3002

RONG-SONG JIH
PHILLIPS LABORATORY
EARTH SCIENCES DIVISION
29 RANDOLPH ROAD
HANSCOM AFB, MA 01731-3010

LAWRENCE LIVERMORE NATIONAL LABORATORY
ATTN: TECHNICAL STAFF (PLS ROUTE)
PO BOX 808, MS L-200
LIVERMORE, CA 94551

LAWRENCE LIVERMORE NATIONAL LABORATORY
ATTN: TECHNICAL STAFF (PLS ROUTE)
PO BOX 808, MS L-221
LIVERMORE, CA 94551

ROBERT GEIL
DOE
PALAIS DES NATIONS, RM D615
GENEVA 10, SWITZERLAND

HENRY GRAY
SMU STATISTICS DEPARTMENT
P.O. BOX 750302
DALLAS, TX 75275-0302

DAVID HARKRIDER
PHILLIPS LABORATORY
EARTH SCIENCES DIVISION
29 RANDOLPH ROAD
HANSCOM AFB, MA 01731-3010

THOMAS HEARN
NEW MEXICO STATE UNIVERSITY
DEPARTMENT OF PHYSICS
LAS CRUCES, NM 88003

DONALD HELMBERGER
CALIFORNIA INSTITUTE OF TECHNOLOGY
DIVISION OF GEOLOGICAL & PLANETARY SCIENCES
SEISMOLOGICAL LABORATORY
PASADENA, CA 91125

ROBERT HERRMANN
ST. LOUIS UNIVERSITY
DEPARTMENT OF EARTH & ATMOSPHERIC SCIENCES
3507 LACLEDE AVENUE
ST. LOUIS, MO 63103

ANTHONY IANNACCHIONE
BUREAU OF MINES
COCHRANE MILL ROAD
PO BOX 18070
PITTSBURGH, PA 15236-9986

THOMAS JORDAN
MASSACHUSETTS INSTITUTE OF TECHNOLOGY
EARTH, ATMOSPHERIC & PLANETARY SCIENCES
77 MASSACHUSETTS AVENUE, 54-918
CAMBRIDGE, MA 02139

LAWRENCE LIVERMORE NATIONAL LABORATORY
ATTN: TECHNICAL STAFF (PLS ROUTE)
PO BOX 808, MS L-207
LIVERMORE, CA 94551

LAWRENCE LIVERMORE NATIONAL LABORATORY
ATTN: TECHNICAL STAFF (PLS ROUTE)
LLNL
PO BOX 808, MS L-175
LIVERMORE, CA 94551

LAWRENCE LIVERMORE NATIONAL LABORATORY
ATTN: TECHNICAL STAFF (PLS ROUTE)
PO BOX 808, MS L-208
LIVERMORE, CA 94551

LAWRENCE LIVERMORE NATIONAL LABORATORY
ATTN: TECHNICAL STAFF (PLS ROUTE)
PO BOX 808, MS L-202
LIVERMORE, CA 94551

LAWRENCE LIVERMORE NATIONAL LABORATORY
ATTN: TECHNICAL STAFF (PLS ROUTE)
PO BOX 808, MS L-195
LIVERMORE, CA 94551

LAWRENCE LIVERMORE NATIONAL LABORATORY
ATTN: TECHNICAL STAFF (PLS ROUTE)
PO BOX 808, MS L-205
LIVERMORE, CA 94551

THORNE LAY
UNIVERSITY OF CALIFORNIA, SANTA CRUZ
EARTH SCIENCES DEPARTMENT
EARTH & MARINE SCIENCE BUILDING
SANTA CRUZ, CA 95064

ANATOLI L. LEVSHIN
DEPARTMENT OF PHYSICS
UNIVERSITY OF COLORADO
CAMPUS BOX 390
BOULDER, CO 80309-0309

DONALD A. LINGER
DNA
6801 TELEGRAPH ROAD
ALEXANDRIA, VA 22310

LOS ALAMOS NATIONAL LABORATORY
ATTN: TECHNICAL STAFF (PLS ROUTE)
PO BOX 1663, MS F659
LOS ALAMOS, NM 87545

LOS ALAMOS NATIONAL LABORATORY
ATTN: TECHNICAL STAFF (PLS ROUTE)
PO BOX 1663, MS F665
LOS ALAMOS, NM 87545

LOS ALAMOS NATIONAL LABORATORY
ATTN: TECHNICAL STAFF (PLS ROUTE)
PO BOX 1663, MS D460
LOS ALAMOS, NM 87545

LOS ALAMOS NATIONAL LABORATORY
ATTN: TECHNICAL STAFF (PLS ROUTE)
PO BOX 1663, MS C335
LOS ALAMOS, NM 87545

GARY MCCARTOR
SOUTHERN METHODIST UNIVERSITY
DEPARTMENT OF PHYSICS
DALLAS, TX 75275-0395

KEITH MCLAUGHLIN
MAXWELL TECHNOLOGIES
P.O. BOX 23558
SAN DIEGO, CA 92123

BRIAN MITCHELL
DEPARTMENT OF EARTH & ATMOSPHERIC SCIENCES
ST. LOUIS UNIVERSITY
3507 LACLEDE AVENUE
ST. LOUIS, MO 63103

RICHARD MORROW
USACDA/IVI
320 21ST STREET, N.W.
WASHINGTON, DC 20451

JOHN MURPHY
MAXWELL TECHNOLOGIES
11800 SUNRISE VALLEY DRIVE SUITE 1212
RESTON, VA 22091

JAMES NI
NEW MEXICO STATE UNIVERSITY
DEPARTMENT OF PHYSICS
LAS CRUCES, NM 88003

JOHN ORCUTT
INSTITUTE OF GEOPHYSICS AND PLANETARY PHYSICS
UNIVERSITY OF CALIFORNIA, SAN DIEGO
LA JOLLA, CA 92093

PACIFIC NORTHWEST NATIONAL LABORATORY
ATTN: TECHNICAL STAFF (PLS ROUTE)
PO BOX 999, MS K6-48
RICHLAND, WA 99352

PACIFIC NORTHWEST NATIONAL LABORATORY
ATTN: TECHNICAL STAFF (PLS ROUTE)
PO BOX 999, MS K7-34
RICHLAND, WA 99352

PACIFIC NORTHWEST NATIONAL LABORATORY
ATTN: TECHNICAL STAFF (PLS ROUTE)
PO BOX 999, MS K6-40
RICHLAND, WA 99352

PACIFIC NORTHWEST NATIONAL LABORATORY
ATTN: TECHNICAL STAFF (PLS ROUTE)
PO BOX 999, MS K5-72
RICHLAND, WA 99352

PACIFIC NORTHWEST NATIONAL LABORATORY
ATTN: TECHNICAL STAFF (PLS ROUTE)
PO BOX 999, MS K5-12
RICHLAND, WA 99352

KEITH PRIESTLEY
DEPARTMENT OF EARTH SCIENCES
UNIVERSITY OF CAMBRIDGE
MADINGLEY RISE, MADINGLEY ROAD
CAMBRIDGE, CB3 OEZ UK

PAUL RICHARDS
COLUMBIA UNIVERSITY
LAMONT-DOHERTY EARTH OBSERVATORY
PALISADES, NY 10964

CHANDAN SAIKIA
WOOODWARD-CLYDE FEDERAL SERVICES
566 EL DORADO ST., SUITE 100
PASADENA, CA 91101-2560

SANDIA NATIONAL LABORATORY
ATTN: TECHNICAL STAFF (PLS ROUTE)
DEPT. 6116
MS 0750, PO BOX 5800
ALBUQUERQUE, NM 87185-0750

SANDIA NATIONAL LABORATORY
ATTN: TECHNICAL STAFF (PLS ROUTE)
DEPT. 9311
MS 1159, PO BOX 5800
ALBUQUERQUE, NM 87185-1159

SANDIA NATIONAL LABORATORY
ATTN: TECHNICAL STAFF (PLS ROUTE)
DEPT. 5736
MS 0655, PO BOX 5800
ALBUQUERQUE, NM 87185-0655

THOMAS SERENO JR.
SCIENCE APPLICATIONS INTERNATIONAL
CORPORATION
10260 CAMPUS POINT DRIVE
SAN DIEGO, CA 92121

PACIFIC NORTHWEST NATIONAL LABORATORY
ATTN: TECHNICAL STAFF (PLS ROUTE)
PO BOX 999, MS K7-22
RICHLAND, WA 99352

PACIFIC NORTHWEST NATIONAL LABORATORY
ATTN: TECHNICAL STAFF (PLS ROUTE)
PO BOX 999, MS K6-84
RICHLAND, WA 99352

FRANK PILOTTE
HQ/AFTAC/TT
1030 S. HIGHWAY A1A
PATRICK AFB, FL 32925-3002

JAY PULLI
RADIX SYSTEMS, INC.
6 TAFT COURT
ROCKVILLE, MD 20850

DAVID RUSSELL
HQ AFTAC/TTR
1030 SOUTH HIGHWAY A1A
PATRICK AFB, FL 32925-3002

SANDIA NATIONAL LABORATORY
ATTN: TECHNICAL STAFF (PLS ROUTE)
DEPT. 5704
MS 0979, PO BOX 5800
ALBUQUERQUE, NM 87185-0979

SANDIA NATIONAL LABORATORY
ATTN: TECHNICAL STAFF (PLS ROUTE)
DEPT. 5791
MS 0567, PO BOX 5800
ALBUQUERQUE, NM 87185-0567

SANDIA NATIONAL LABORATORY
ATTN: TECHNICAL STAFF (PLS ROUTE)
DEPT. 5704
MS 0655, PO BOX 5800
ALBUQUERQUE, NM 87185-0655

SANDIA NATIONAL LABORATORY
ATTN: TECHNICAL STAFF (PLS ROUTE)
DEPT. 6116
MS 0750, PO BOX 5800
ALBUQUERQUE, NM 87185-0750

AVI SHAPIRA
SEISMOLOGY DIVISION
THE INSTITUTE FOR PETROLEUM RESEARCH AND
GEOPHYSICS
P.O.B. 2286, NOLON 58122 ISRAEL

ROBERT SHUMWAY
410 MRAK HALL
DIVISION OF STATISTICS
UNIVERSITY OF CALIFORNIA
DAVIS, CA 95616-8671

DAVID SIMPSON
IRIS
1616 N. FORT MEYER DRIVE
SUITE 1050
ARLINGTON, VA 22209

BRIAN SULLIVAN
BOSTON COLLEGE
INSITUTE FOR SPACE RESEARCH
140 COMMONWEALTH AVENUE
CHESTNUT HILL, MA 02167

NAFI TOKSOZ
EARTH RESOURCES LABORATORY, M.I.T.
42 CARLTON STREET, E34-440
CAMBRIDGE, MA 02142

GREG VAN DER VINK
IRIS
1616 N. FORT MEYER DRIVE
SUITE 1050
ARLINGTON, VA 22209

TERRY WALLACE
UNIVERSITY OF ARIZONA
DEPARTMENT OF GEOSCIENCES
BUILDING #77
TUCSON, AZ 85721

JAMES WHITCOMB
NSF
NSF/ISC OPERATIONS/EAR-785
4201 WILSON BLVD., ROOM785
ARLINGTON, VA 22230

JIAKANG XIE
COLUMBIA UNIVERSITY
LAMONT DOHERTY EARTH OBSERVATORY
ROUTE 9W
PALISADES, NY 10964

OFFICE OF THE SECRETARY OF DEFENSE
DDR&E
WASHINGTON, DC 20330

TACTEC
BATTELLE MEMORIAL INSTITUTE
505 KING AVENUE
COLUMBUS, OH 43201 (FINAL REPORT)

MATTHEW SIBOL
ENSCO, INC.
445 PINEDA COURT
MELBOURNE, FL 32940

JEFFRY STEVENS
MAXWELL TECHNOLOGIES
P.O. BOX 23558
SAN DIEGO, CA 92123

DAVID THOMAS
ISEE
29100 AURORA ROAD
CLEVELAND, OH 44139

LAWRENCE TURNBULL
ACIS
DCI/ACIS
WASHINGTON, DC 20505

FRANK VERNON
UNIVERSITY OF CALIFORNIA, SAN DIEGO
SCRIPPS INSTITUTION OF OCEANOGRAPHY IGPP, 0225
9500 GILMAN DRIVE
LA JOLLA, CA 92093-0225

DANIEL WEILL
NSF
EAR-785
4201 WILSON BLVD., ROOM 785
ARLINGTON, VA 22230

RU SHAN WU
UNIVERSITY OF CALIFORNIA SANTA CRUZ
EARTH SCIENCES DEPT.
1156 HIGH STREET
SANTA CRUZ, CA 95064

JAMES E. ZOLLWEG
BOISE STATE UNIVERSITY
GEOSCIENCES DEPT.
1910 UNIVERSITY DRIVE
BOISE, ID 83725

DEFENSE TECHNICAL INFORMATION CENTER
8725 JOHN J. KINGMAN ROAD
FT BELVOIR, VA 22060-6218 (2 COPIES)

PHILLIPS LABORATORY
ATTN: XPG
29 RANDOLPH ROAD
HANSCOM AFB, MA 01731-3010

PHILLIPS LABORATORY
ATTN: GPE
29 RANDOLPH ROAD
HANSCOM AFB, MA 01731-3010

PHILLIPS LABORATORY
ATTN: TSML
5 WRIGHT STREET
HANSCOM AFB, MA 01731-3004

PHILLIPS LABORATORY
ATTN: PL/SUL
3550 ABERDEEN AVE SE
KIRTLAND, NM 87117-5776 (2 COPIES)